

Secondary particles in the Galaxy: the role of cross sections

Fiorenza Donato

Torino University & INFN

Paris 05.12.2022 - "Cosmic Ray in the Multi-Messenger Era"

CRs in the Galaxy

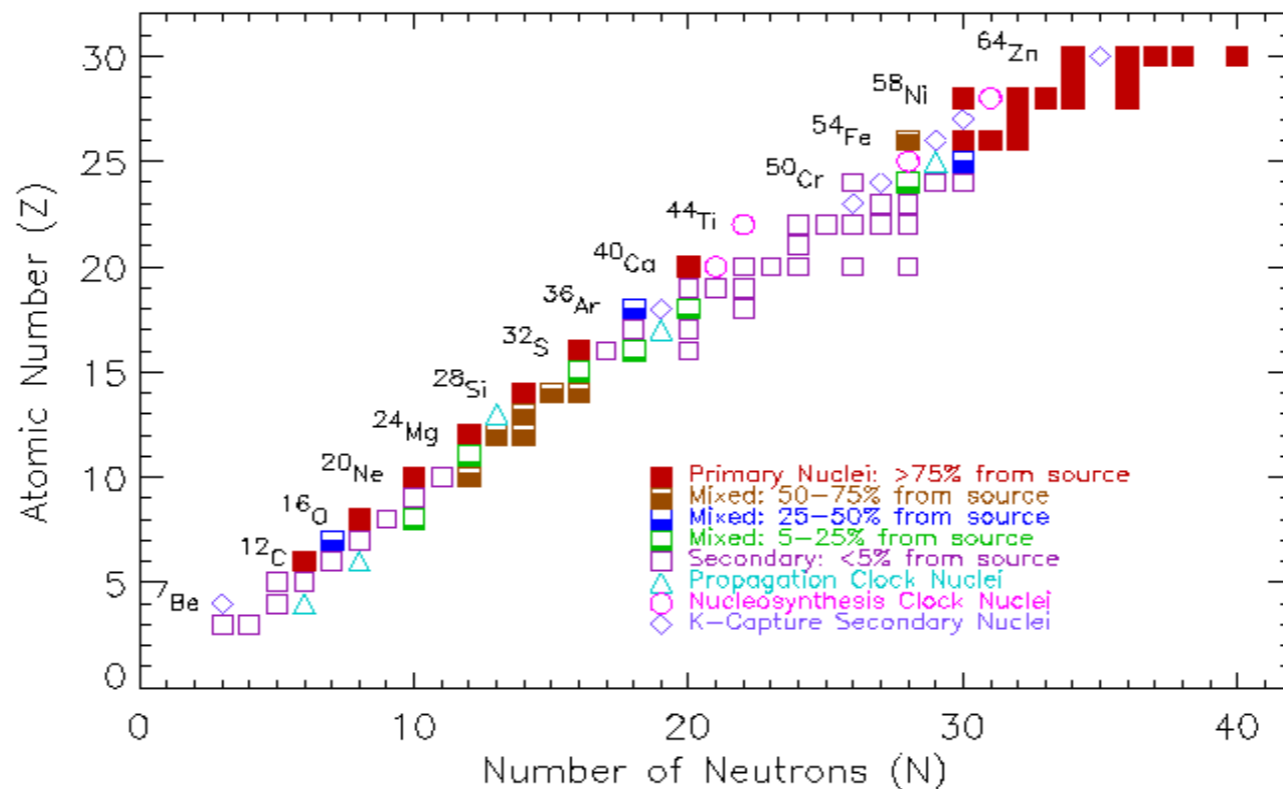
Primaries: produced in the sources (SNR and Pulsars)

H, He, CNO, Fe; e^- , e^+ ; possibly e^+ , p^- , d^- from Dark Matter annihilation

Secondaries: produced by spallation of primary CRs (p, He, C, O, Fe) on the interstellar medium (ISM): Li, Be, B, sub-Fe, [...], (radioactive) isotopes ; e^+ , p^- , d^-

Primaries = present in sources:
 Nuclei: H, He, CNO, Fe; e^- , (e^+) in SNR (& pulsars)
 e^+ , p^+ , d^+ from Dark Matter annihilation

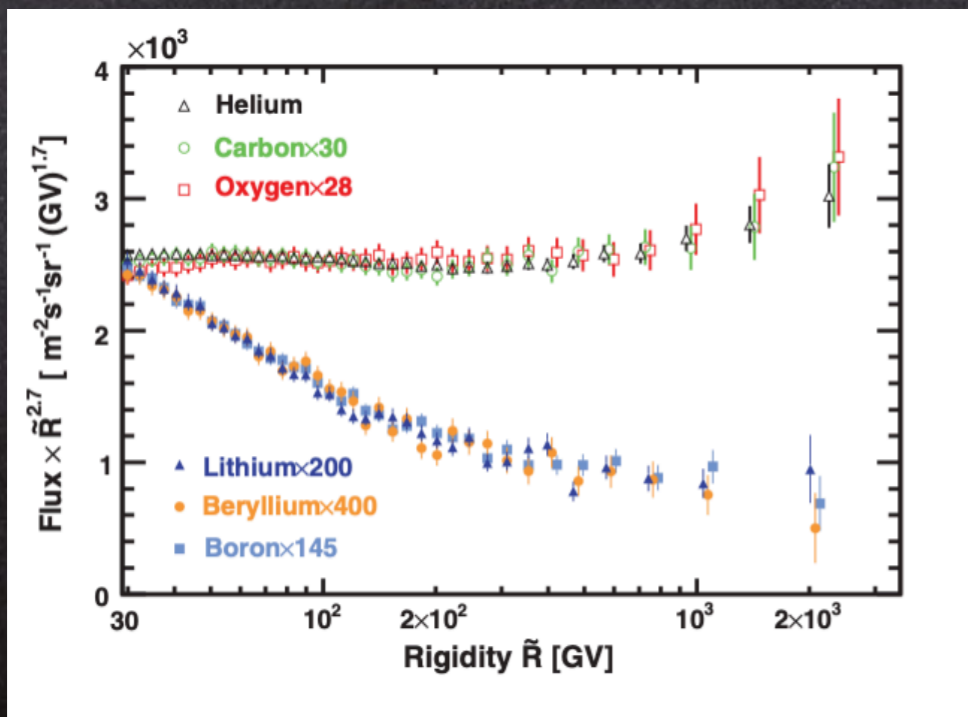
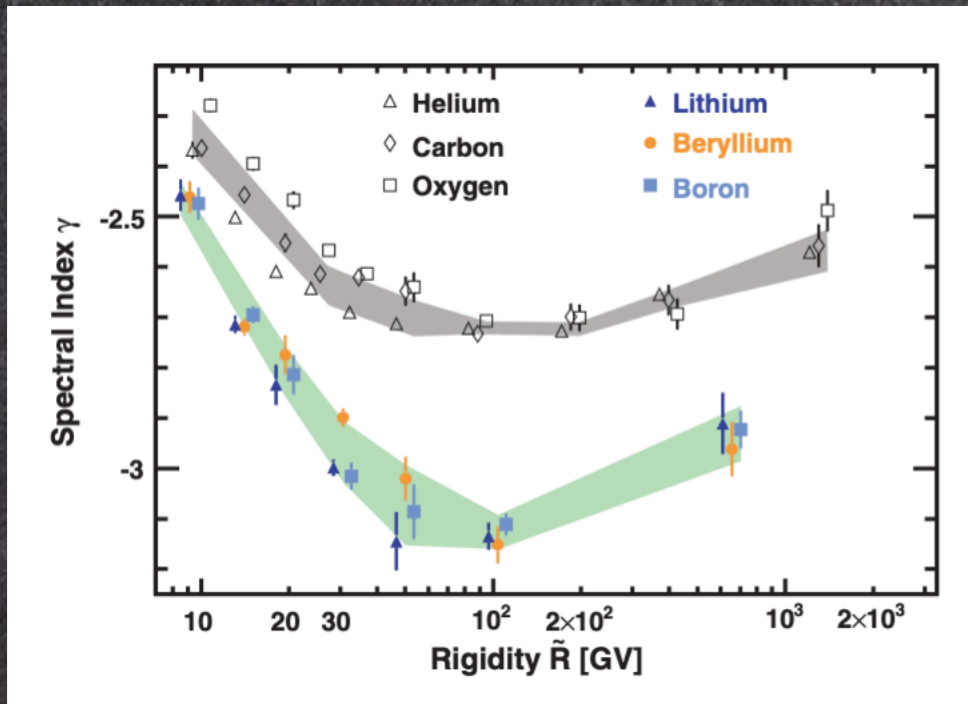
Secondaries = NOT present in sources, thus produced by
 spallation of primary CRs (p, He, C, O, Fe) on ISM
 Nuclei: LiBeB, sub-Fe, ... ;
 e^+ , p^+ , d^+ ; ... from inelastic scatterings



The spectrum of secondary fluxes

See talk by Paolo Zucccon

The rigidity dependence of Li, Be and B are nearly identical, but different from the primary He, C and O (and also p).

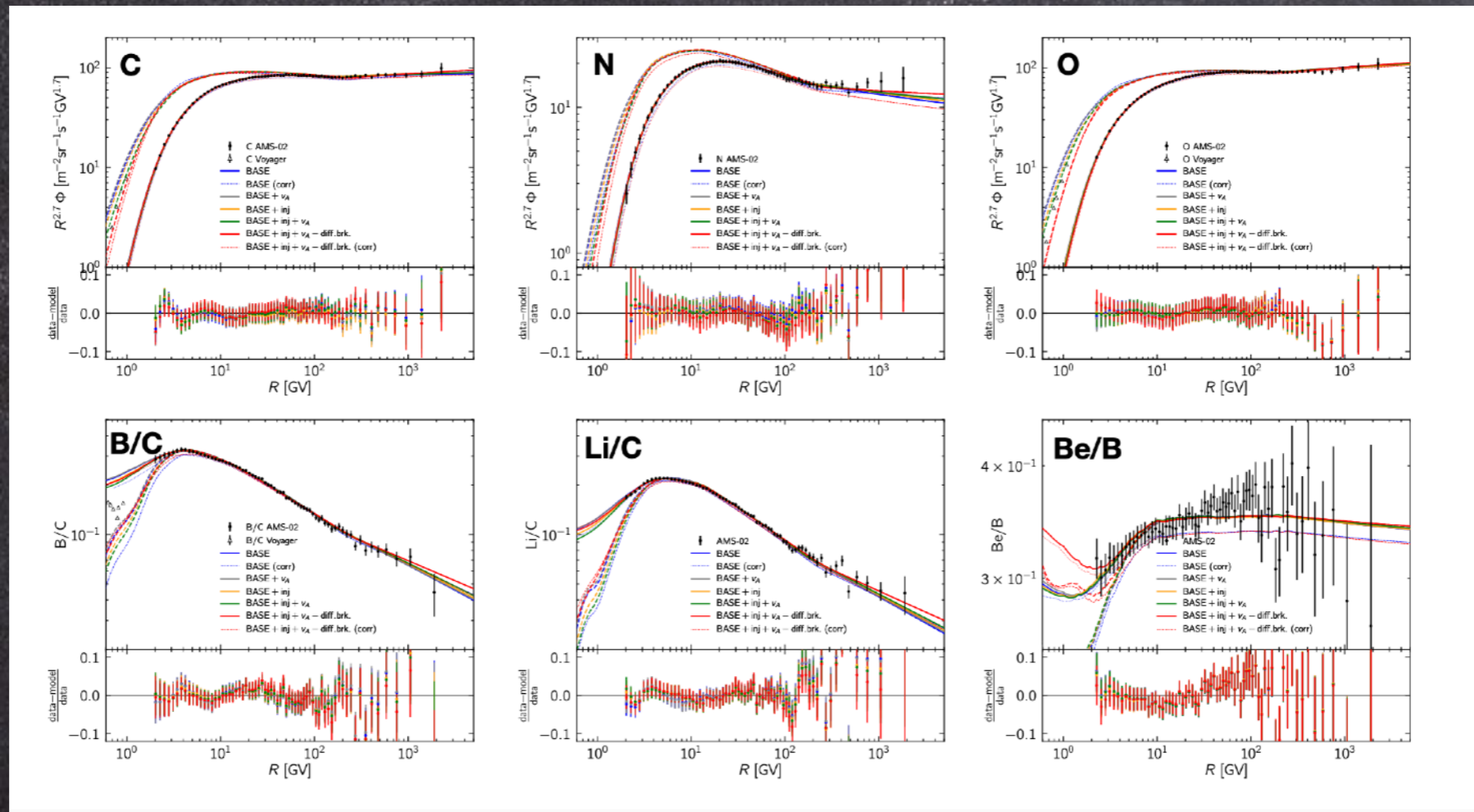


Li, Be, B fluxes measured by Pamela and AMS show an identical hardening w.r.t. energy above 200 GV. The spectral index of secondaries hardens 0.13 ± 0.03 more than for primaries

Propagation models vs data

Korsmeier & Cuoco, PRD 2021

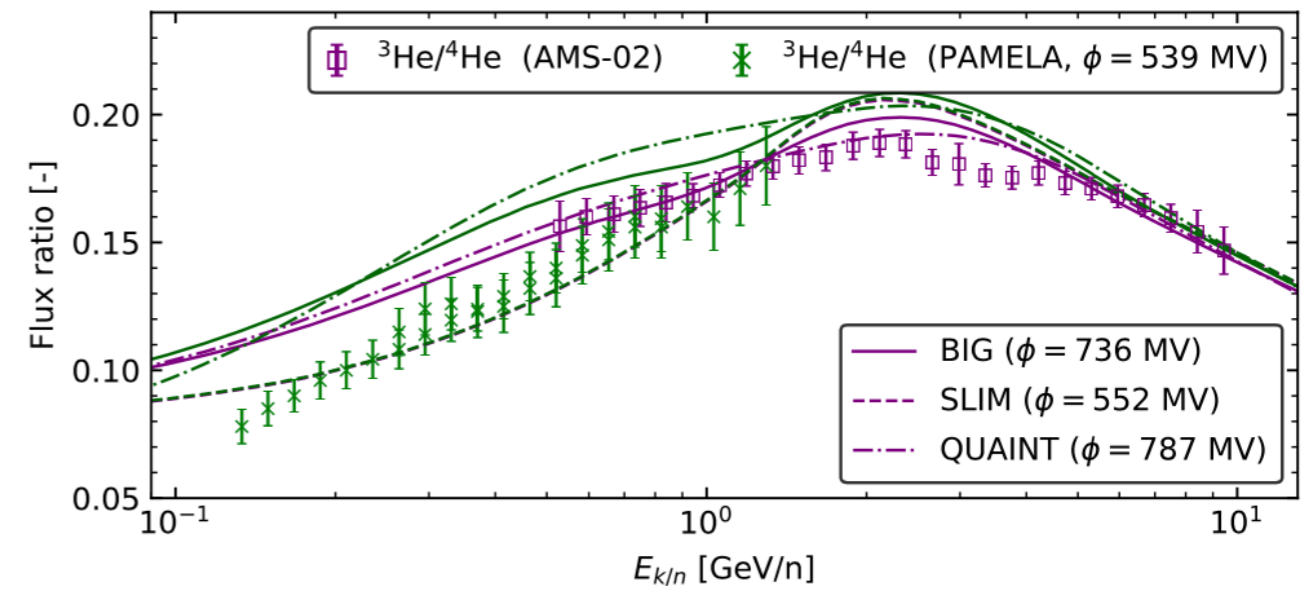
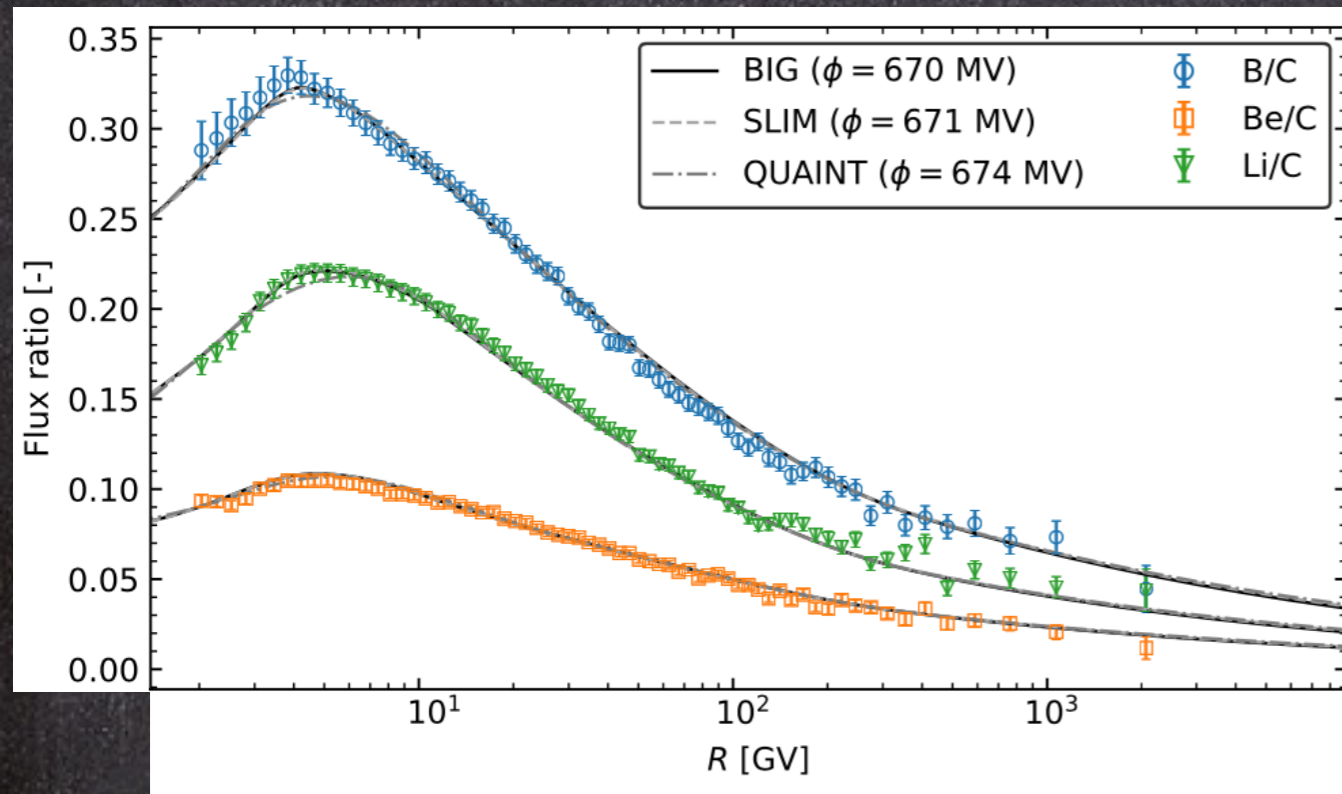
Several propagation models are tested



Fragmentation cross section uncertainties currently prevent a better understanding of CR propagation

Propagation models vs data

Weinrich+ A&A 2020



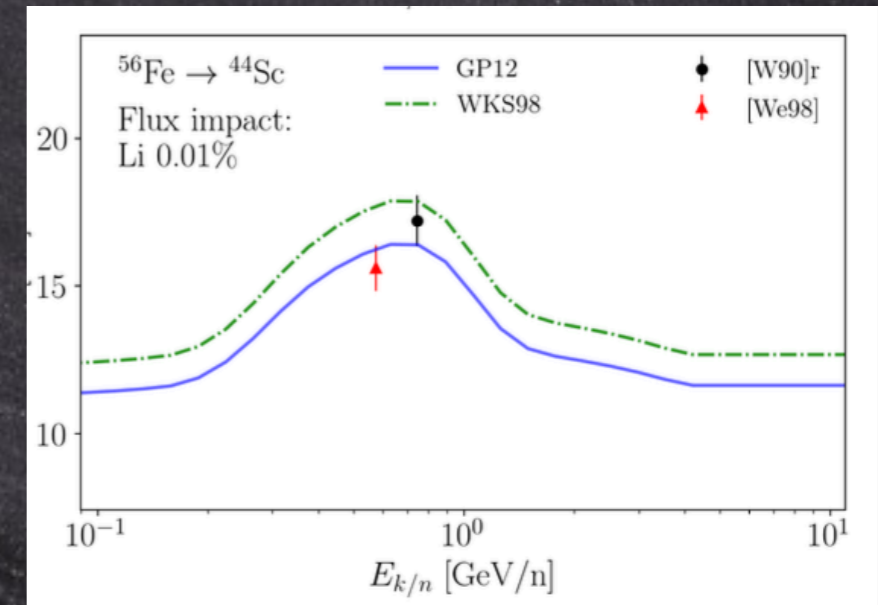
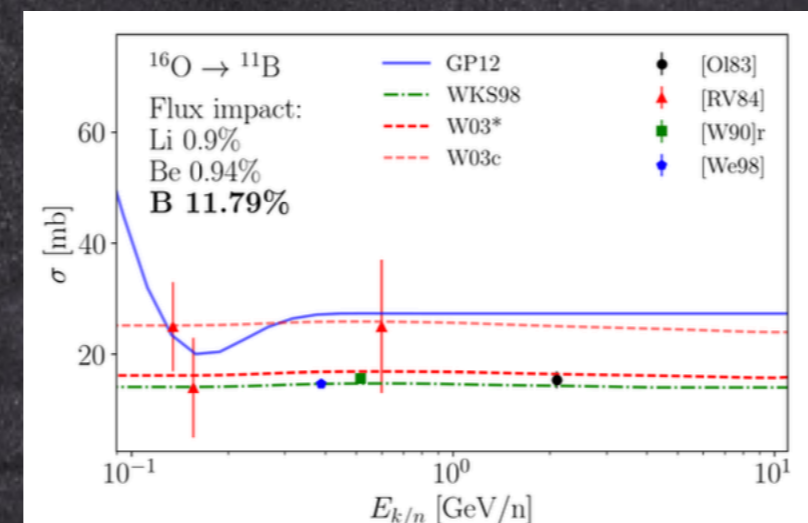
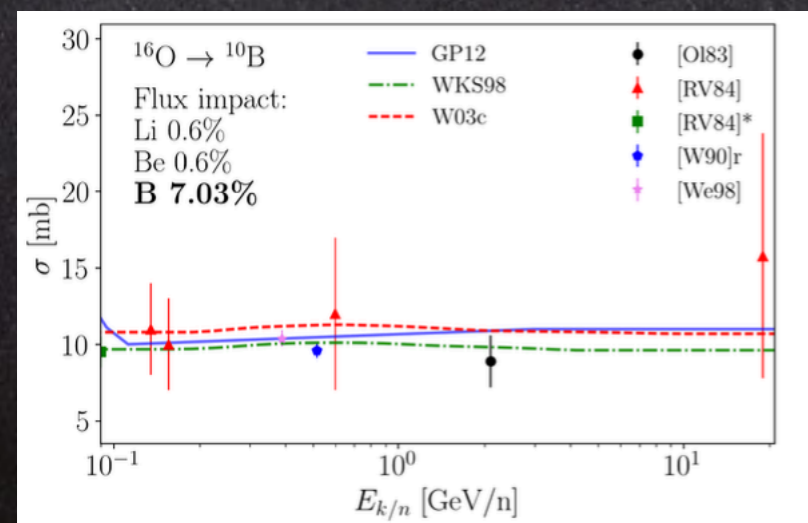
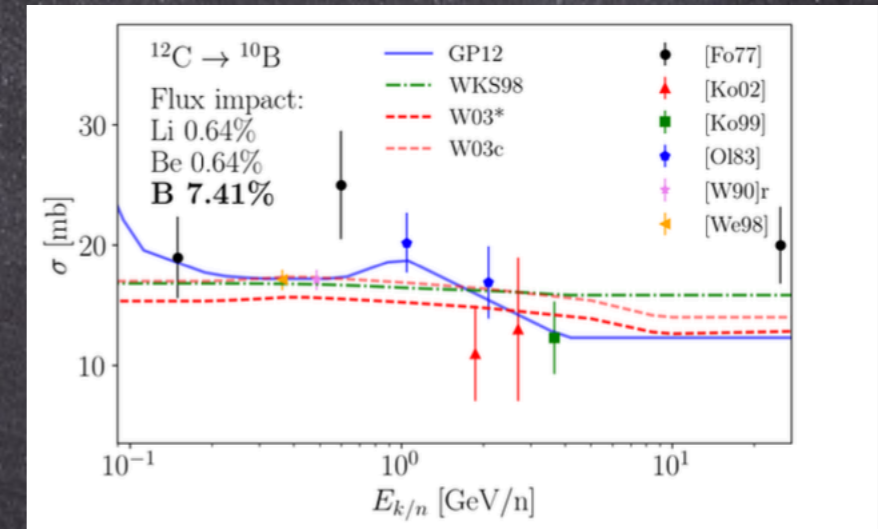
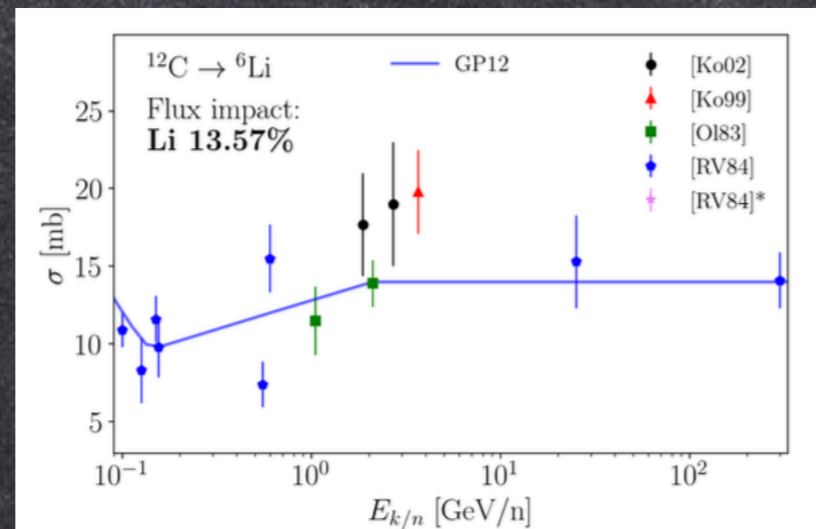
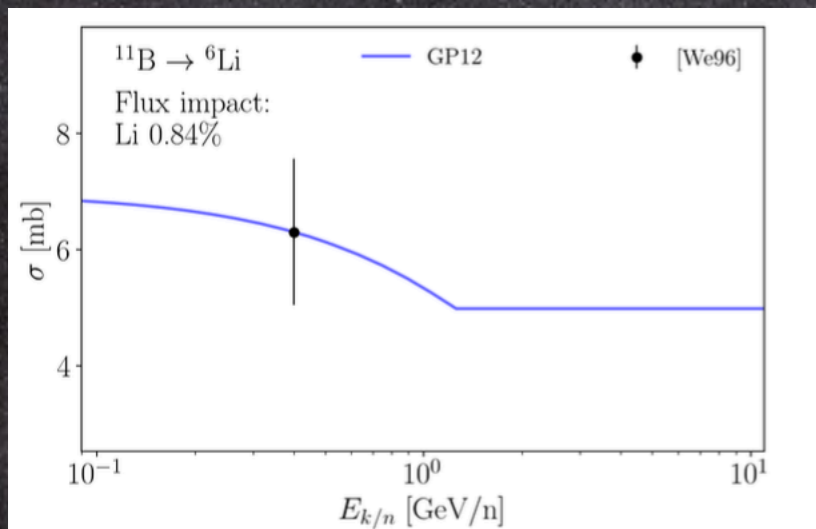
Data on secondary/primary species are well described by propagation model with diffusive coefficient power index $\delta = 0.50 \pm 0.03$.

Convection + reaccelerating, or pure diffusion both work.

Cross sections for Galactic cosmic rays

Data driven parameterizations (Silberberg & Tsao), semi-empirical formulae (Webber+), parametric formulae/direct fit to the data (Galprop), MonteCarlo codes (Fluka, Geant, ...)

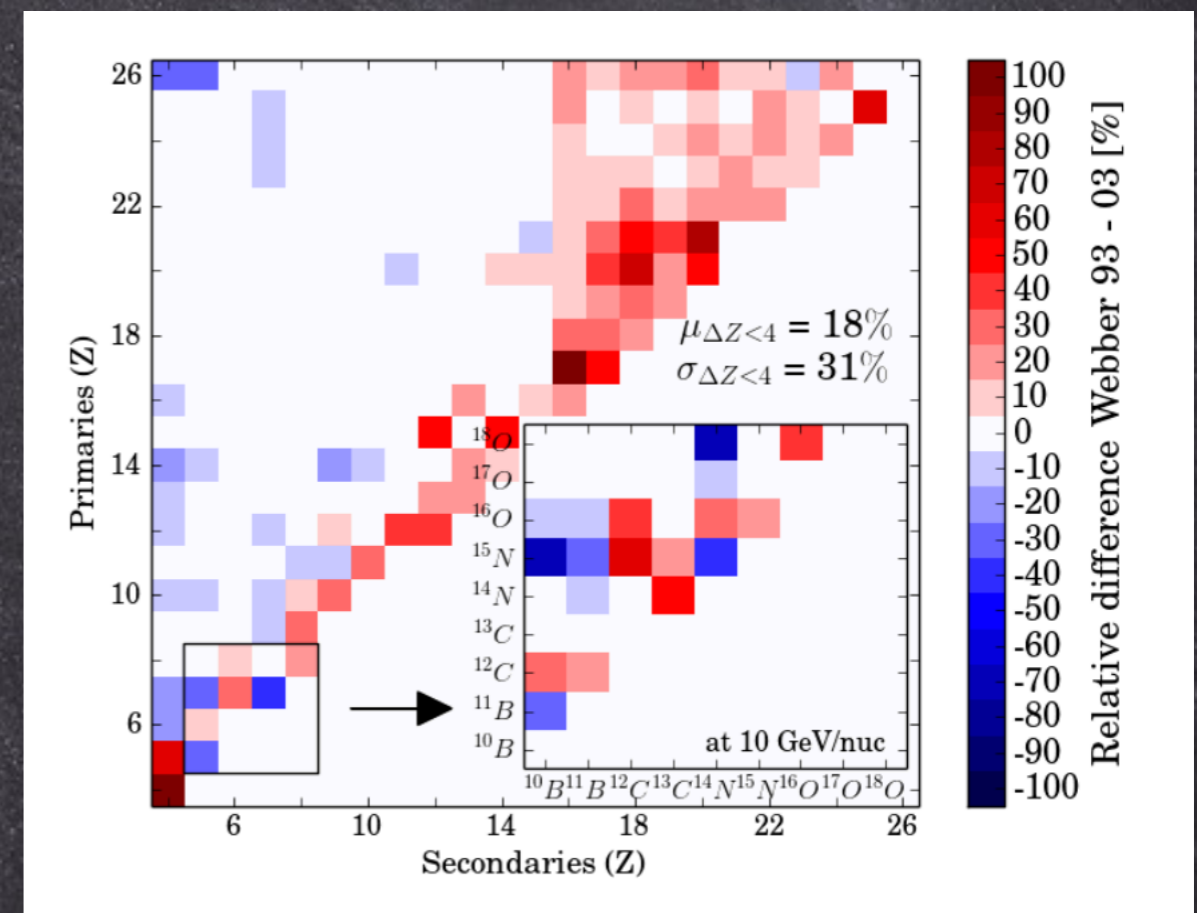
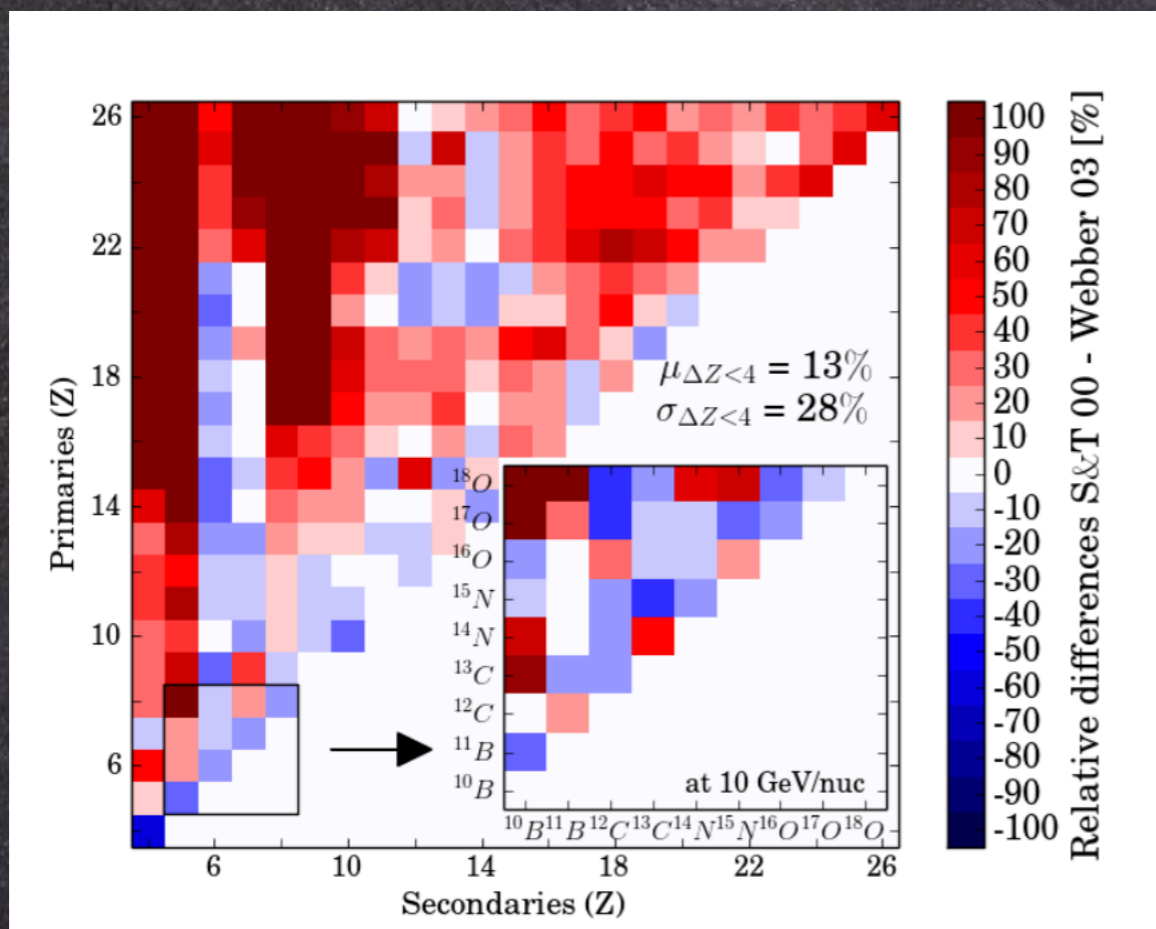
Genolini, Moskalenko, Maurin, Unger PRC 2018



Differences in the XS parameterizations

Genolini, Putze, Salati, Serpico A&A 2015

Differences in one parameterization wrt a benchmark model



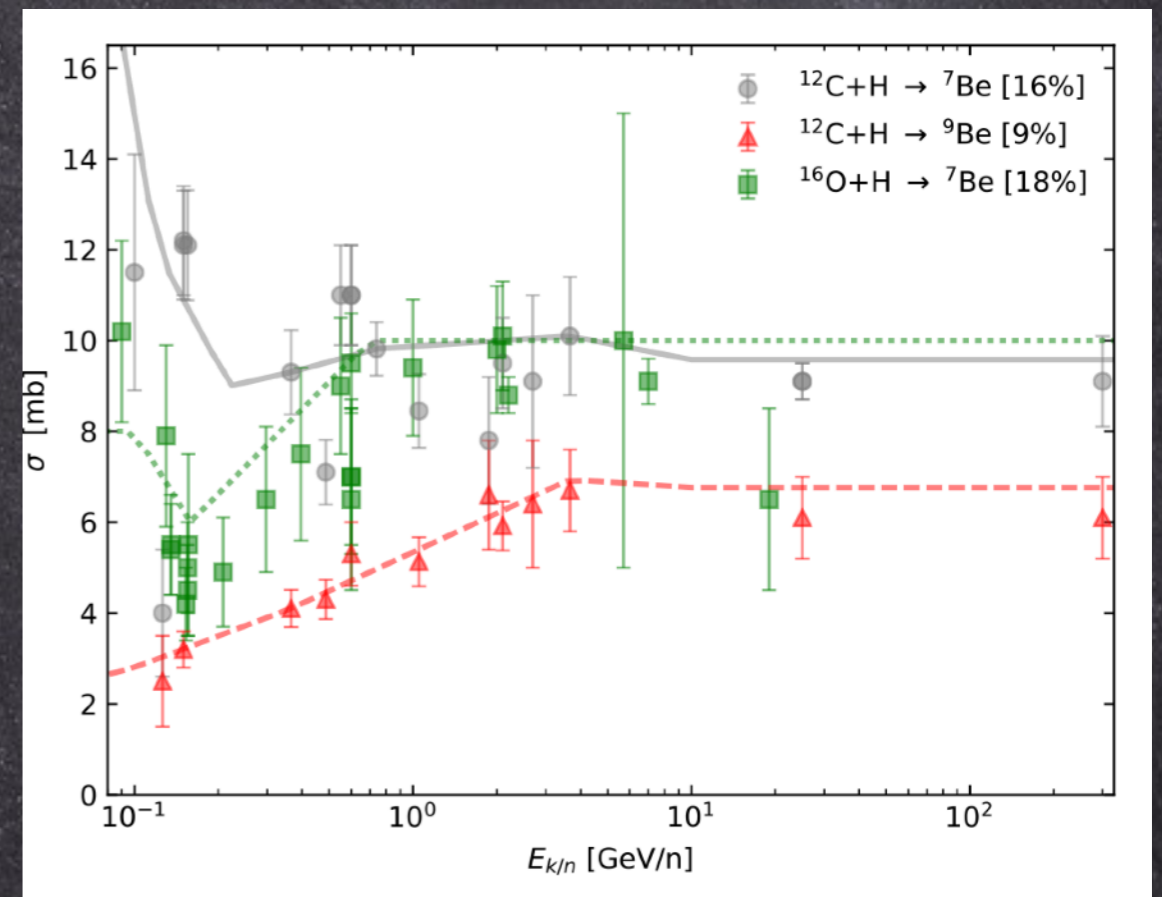
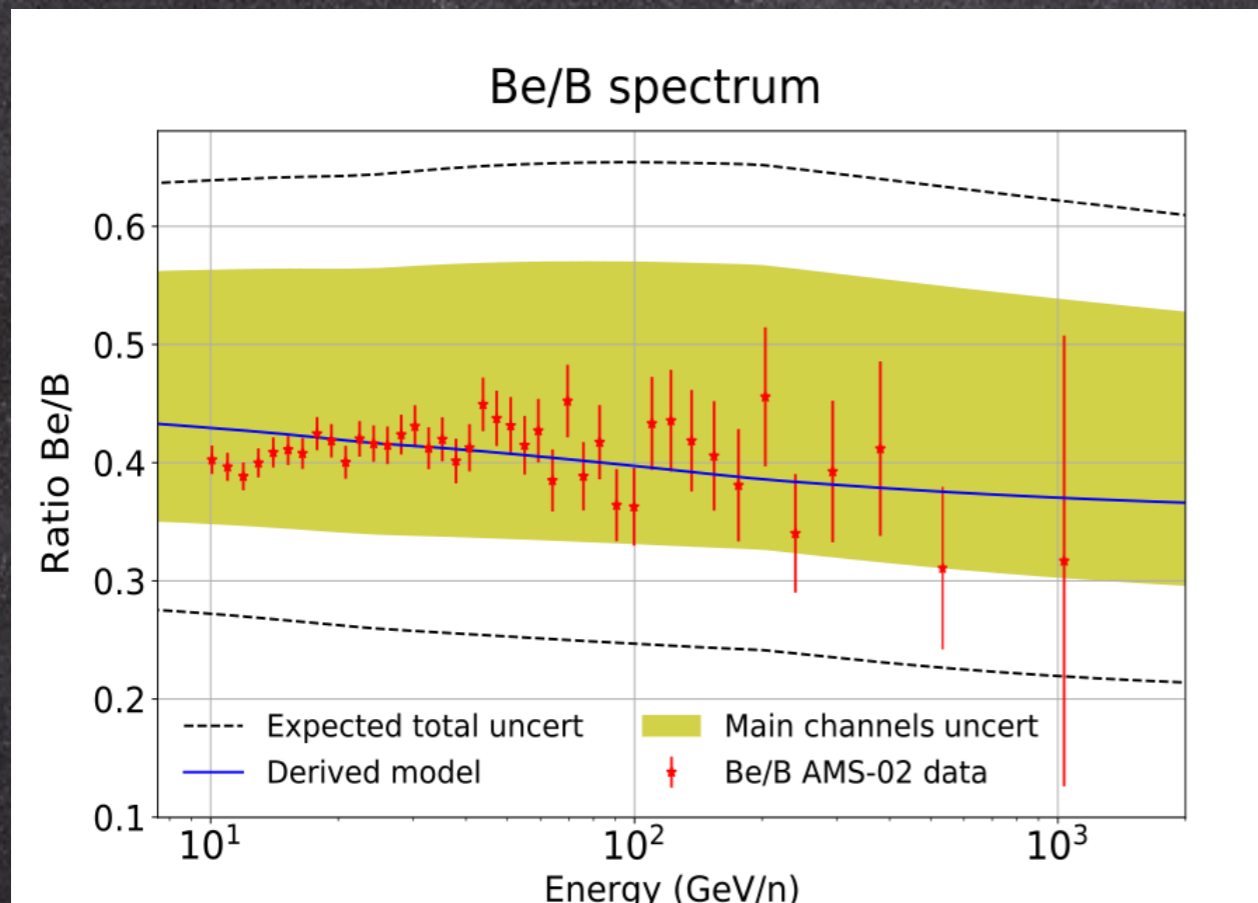
Even with the same, although scarce data, interpretation may be different

Fragmentation cross sections

They matter in both directions: as a loss term for progenitors, as a source term for daughters

De La Torre Luquet+ JCAP 2021

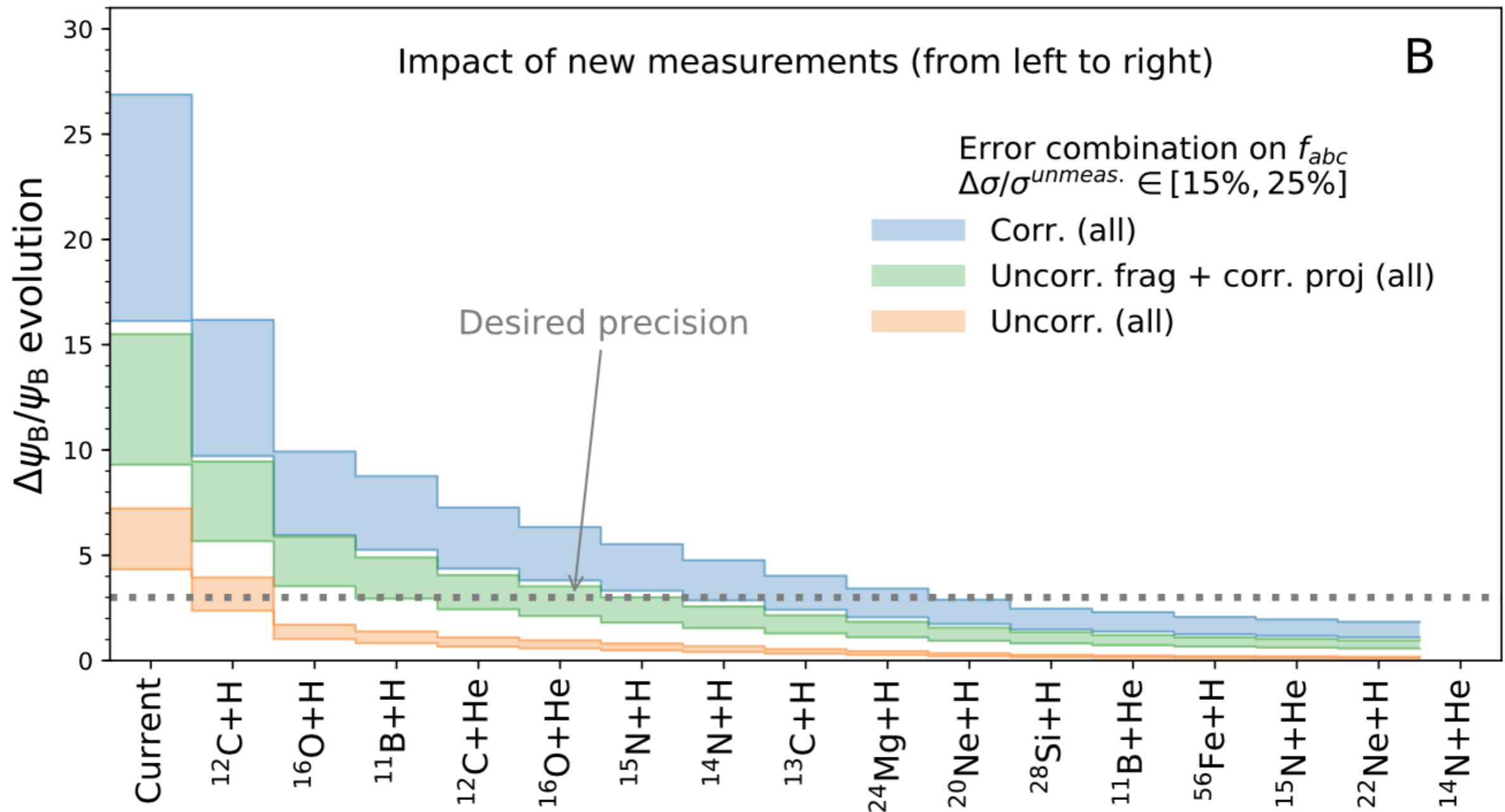
Weinrich+ A&A 2021



Probably the most limiting aspect now
Dedicated campaigns are needed (LHCb, NA61, Amber/Compass, ...)

Most relevant physics cases

Improve Boron production cross sections



Antimatter

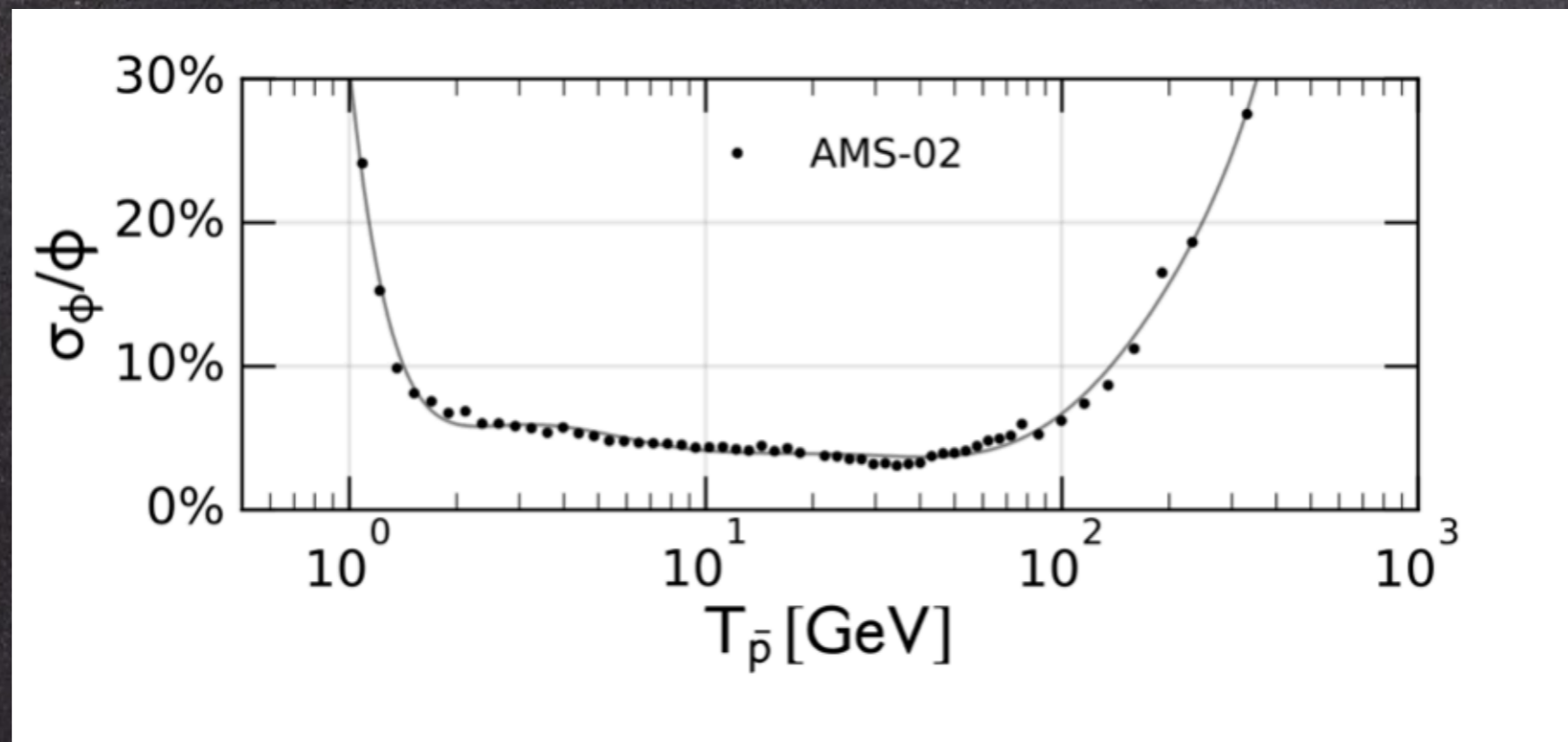
in the Galaxy

Antiproton production by inelastic scatterings

Korsmeier, FD, Di Mauro PRD 2018

$$q_{ij}(T_{\bar{p}}) = \int_{T_{\text{th}}}^{\infty} dT_i 4\pi n_{\text{ISM},j} \phi_i(T_i) \frac{d\sigma_{ij}}{dT_{\bar{p}}}(T_i, T_{\bar{p}}). \quad \frac{d\sigma_{ij}}{dT_{\bar{p}}}(T, T_{\bar{p}}) = p_{\bar{p}} \int d\Omega \sigma_{\text{inv}}^{(ij)}(T_i, T_{\bar{p}}, \theta).$$

Data from space are very precise



We need cross sections at <3%

Recent data at collider

$pp \rightarrow \bar{p} + X$

NA61 (Aduszkiewicz Eur. Phys. J. C77 (2017))

$\sqrt{s} = 7.7, 8.8, 12.3$ and 17.3 GeV

$T_p = 31, 40, 80, 158$ GeV

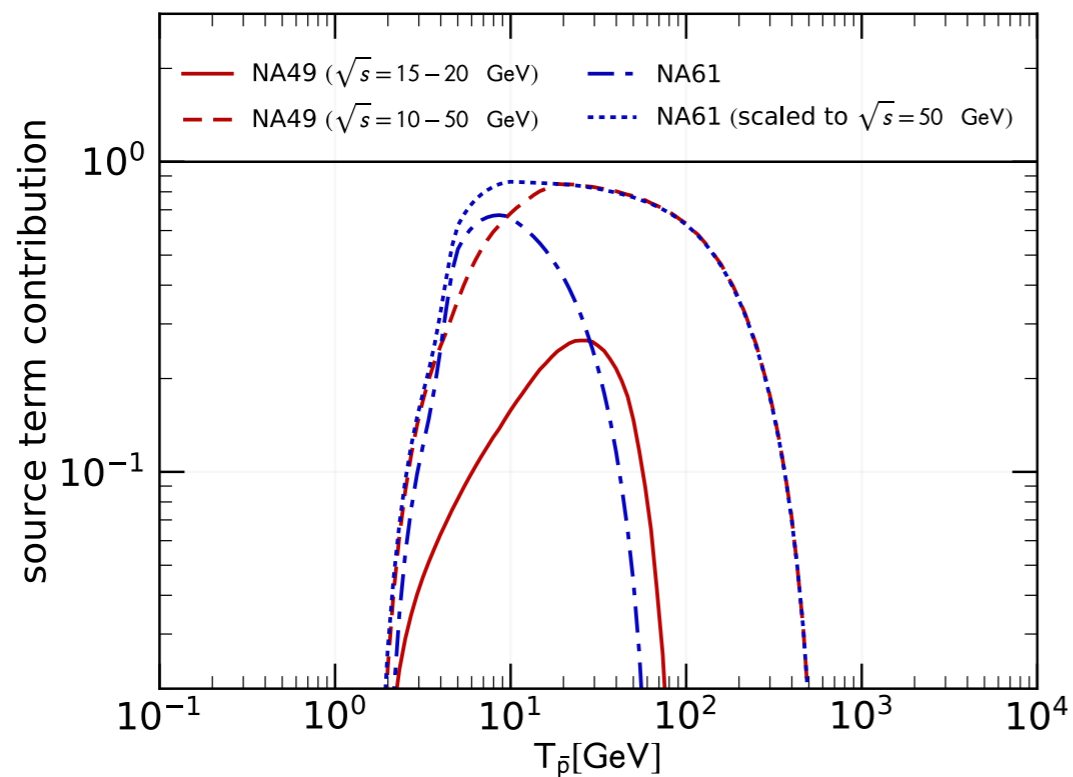
$p\text{He} \rightarrow \bar{p} + X$

LHCb (Graziani et al. Moriond 2017)

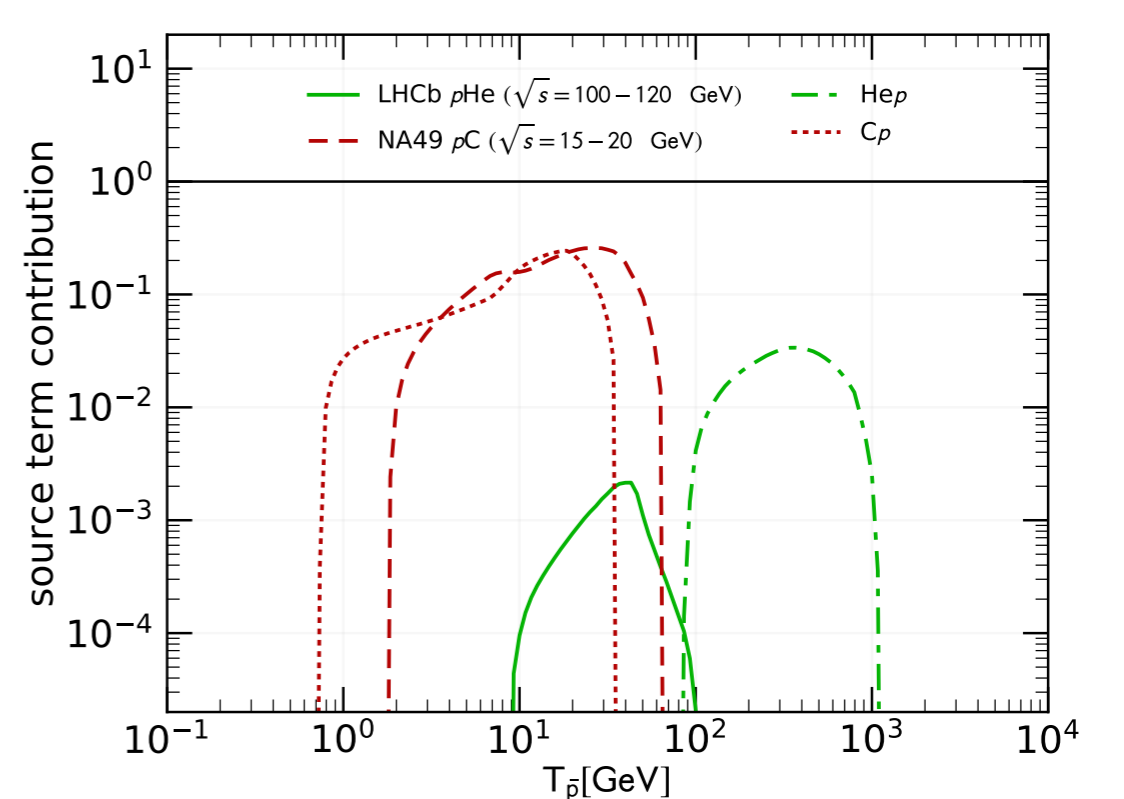
$\sqrt{s} = 110$ GeV

$T_p = 6.5$ TeV

Fraction of the pp source term covered by the kinematical parameters space



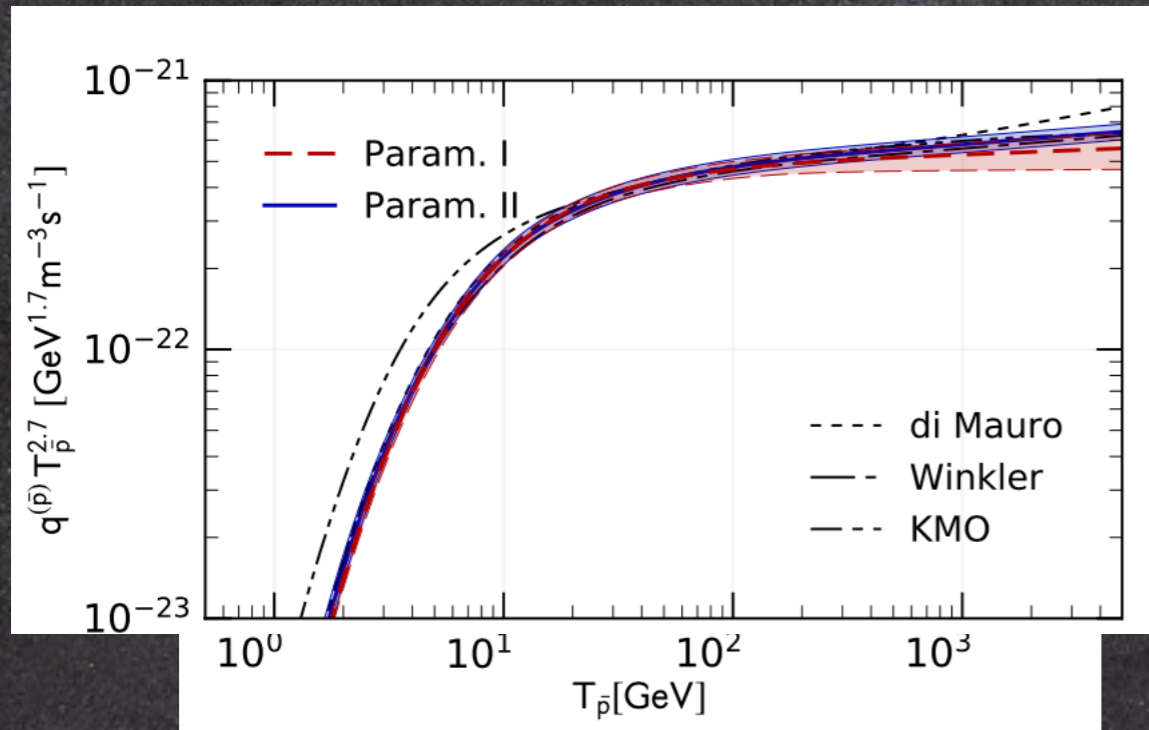
Fraction of the p -nucleus source term covered by the kinematical parameters space



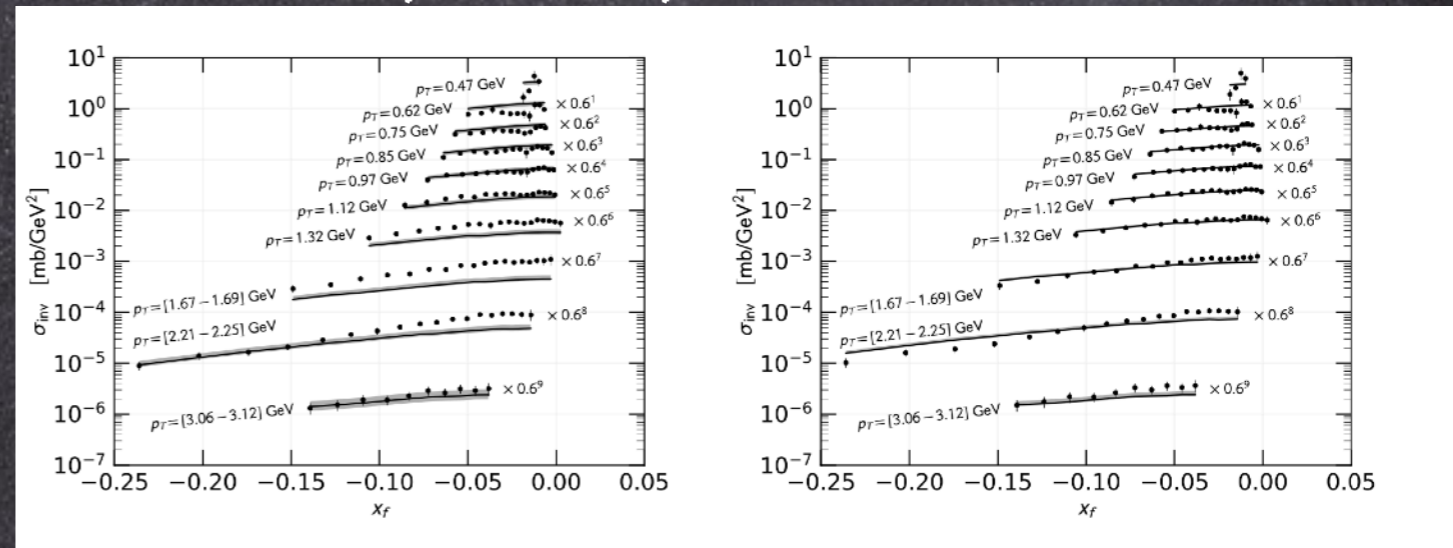
The antiproton source spectrum

Korsmeier, FD, Di Mauro, PRD 2018

$pp \rightarrow p^- X$ source term



LHCb $pHe \rightarrow p^- X$ data & our fit

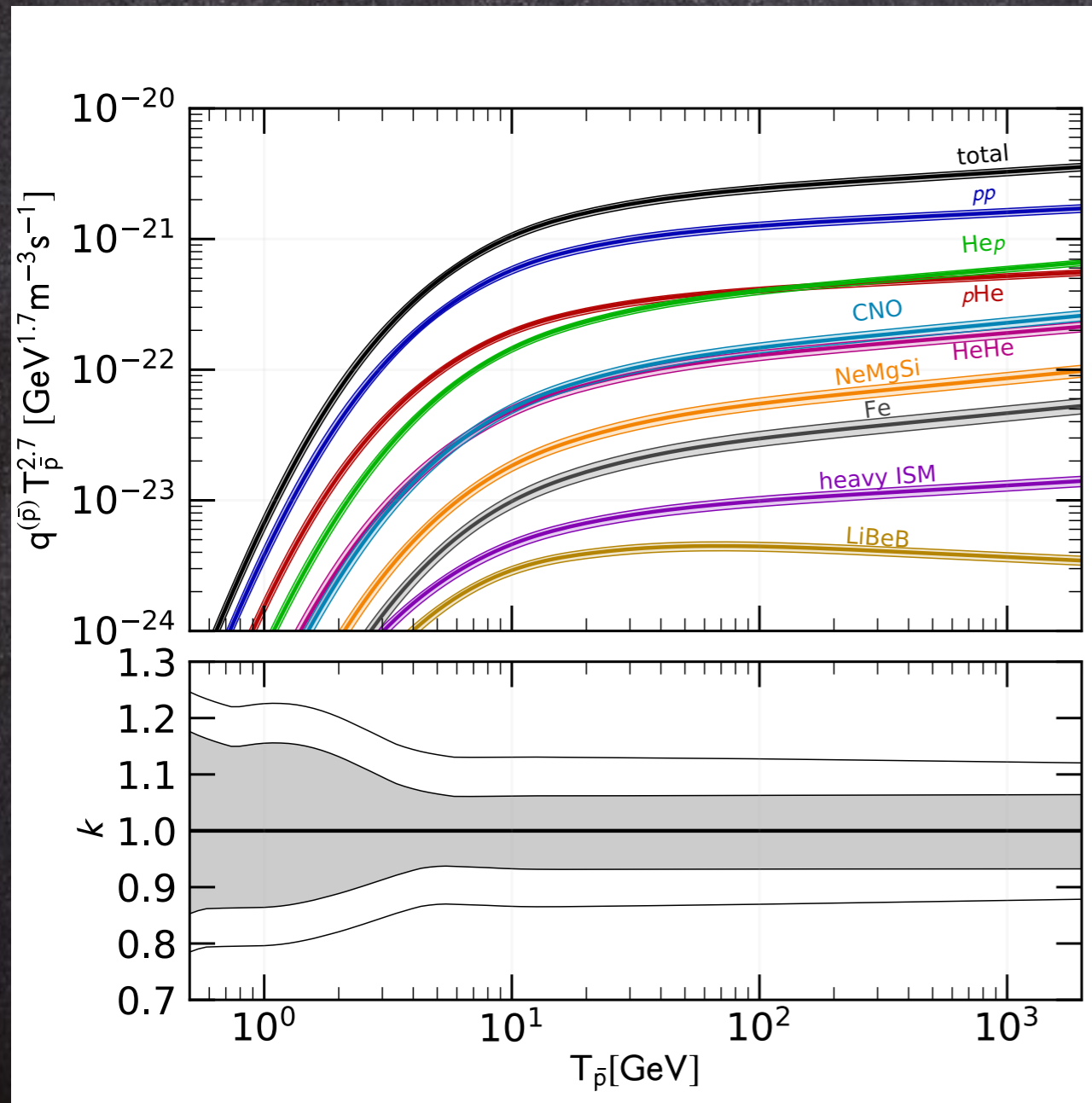


The effect of LHCb data is to select a high energy trend of the $p\bar{p}$ source.

A harder trend is preferred.

Effects on the total pbar production

Korsmeier, FD, Di Mauro, 1802.03030, PRD 2018



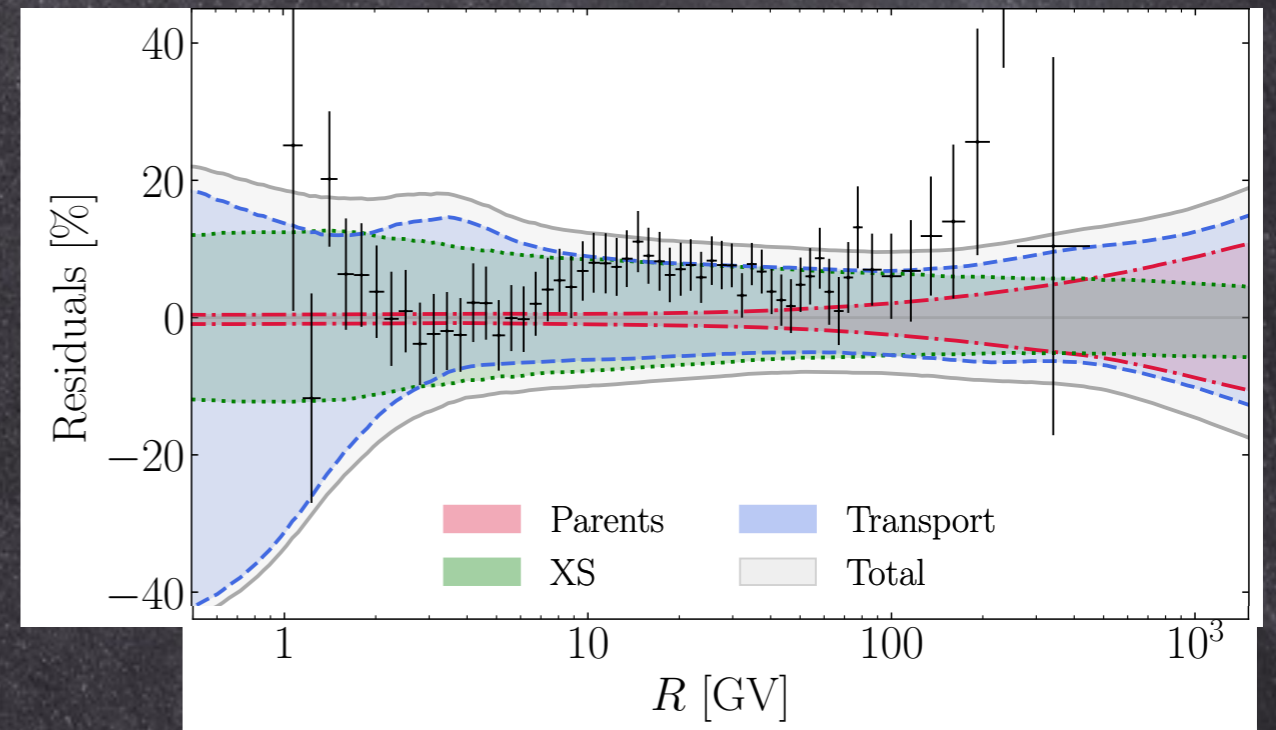
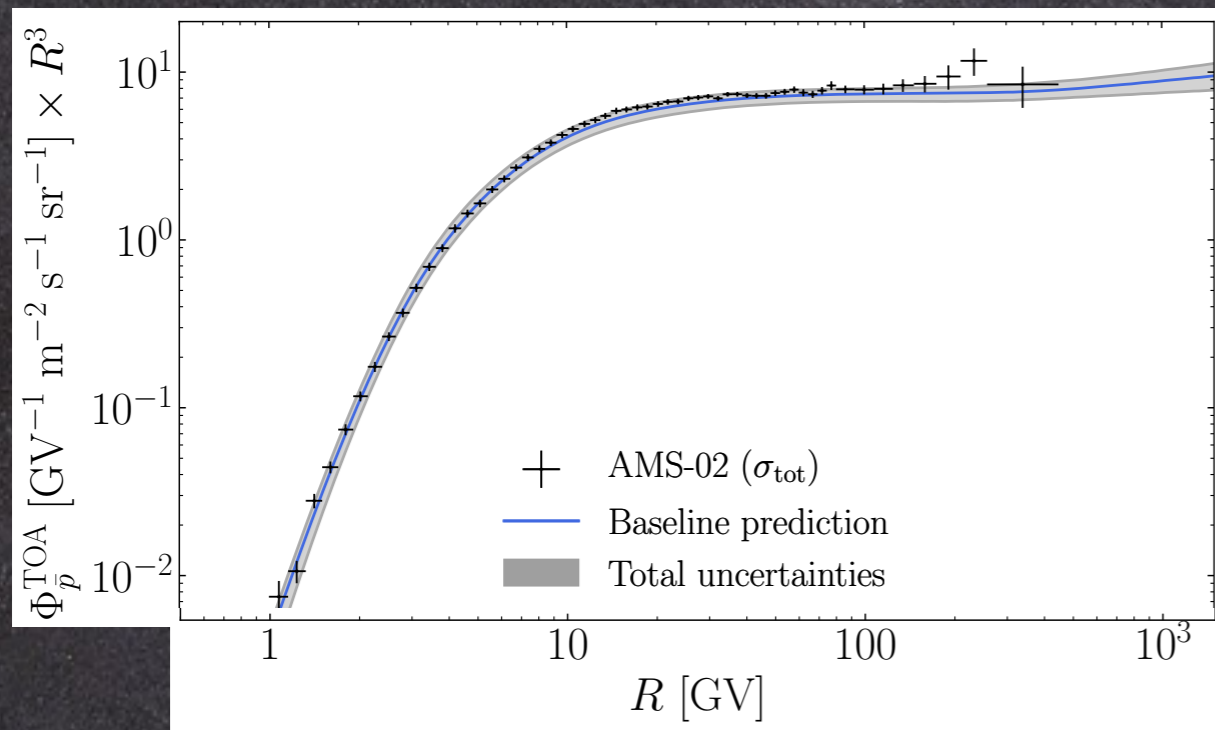
Result with uncertainties in the hyperon correction and isospin violation

The antiproton source term is affected by uncertainties of $\pm 10\%$ from cross sections.

Higher uncertainties at very low energies

AMS-02 antiprotons are consistent with a secondary astrophysical origin

M. Boudaud, Y. Genolini, L. Derome, J.Lavalle,
D.Maurin, P. Salati, P.D. Serpico PRD 2020



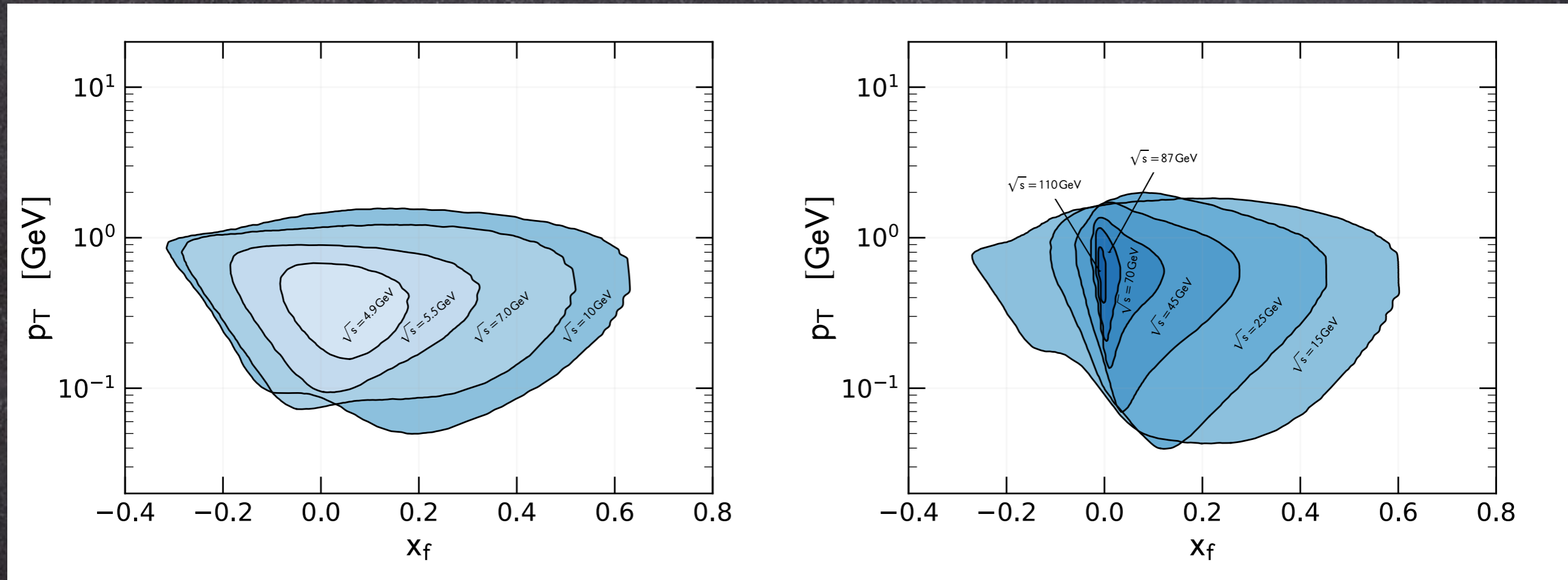
Secondary pbar flux is predicted consistent with AMS-02 data

A dark matter contribution would come as a tiny effect

Transport and cross section uncertainties are comparable

For next generation experiments

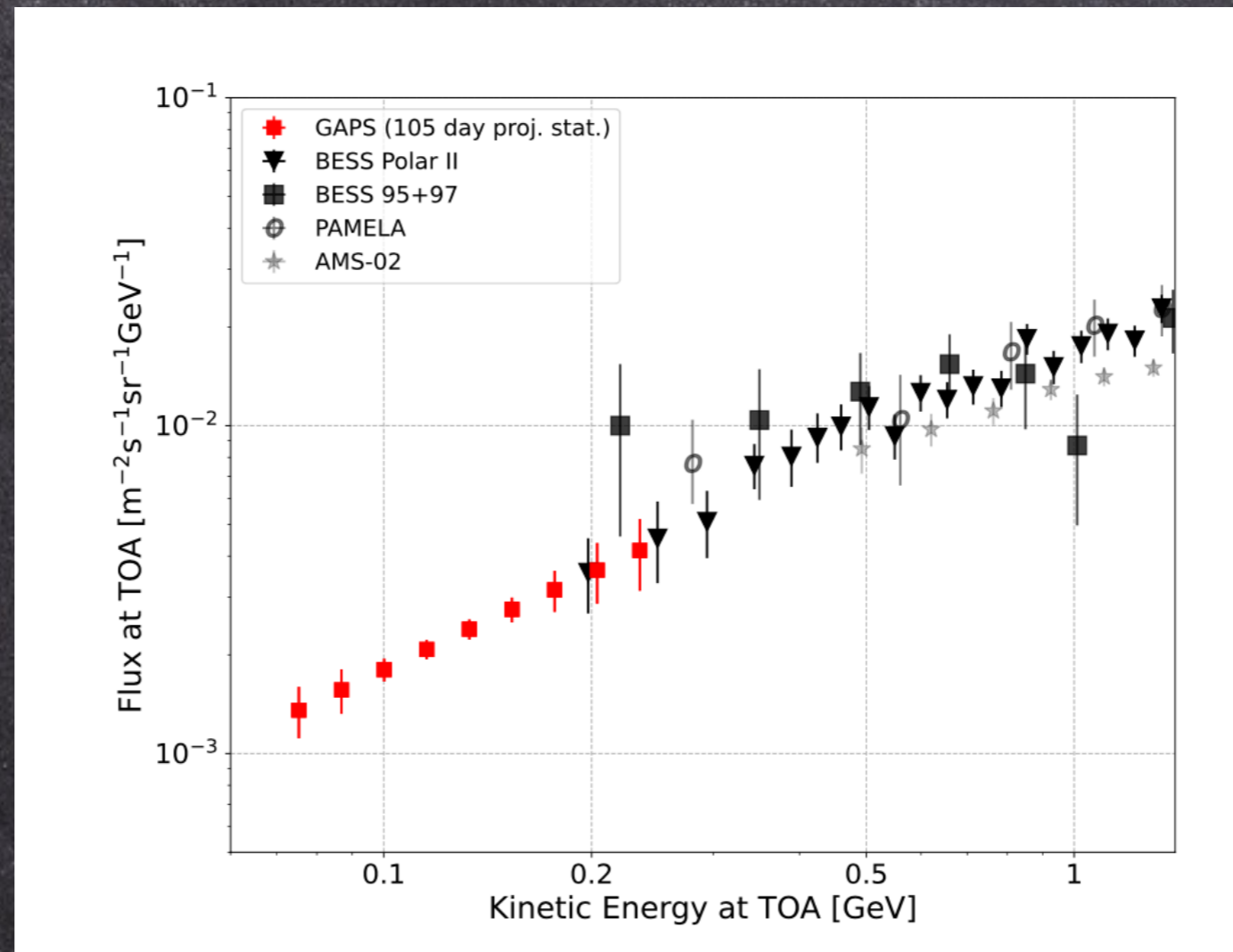
Korsmeier, FD, Di Mauro, 1802.03030, PRD 2018



AMS-02 accuracy is reached if $pp \rightarrow p\bar{b}$ cross section is measured with 3% accuracy inside the regions, 30% outside.

The new frontier of cosmic antiprotons: low energies by GAPS

Rogers et al. (GAPS Coll.) *Astrop. Phys.* 2023, 2206.12991



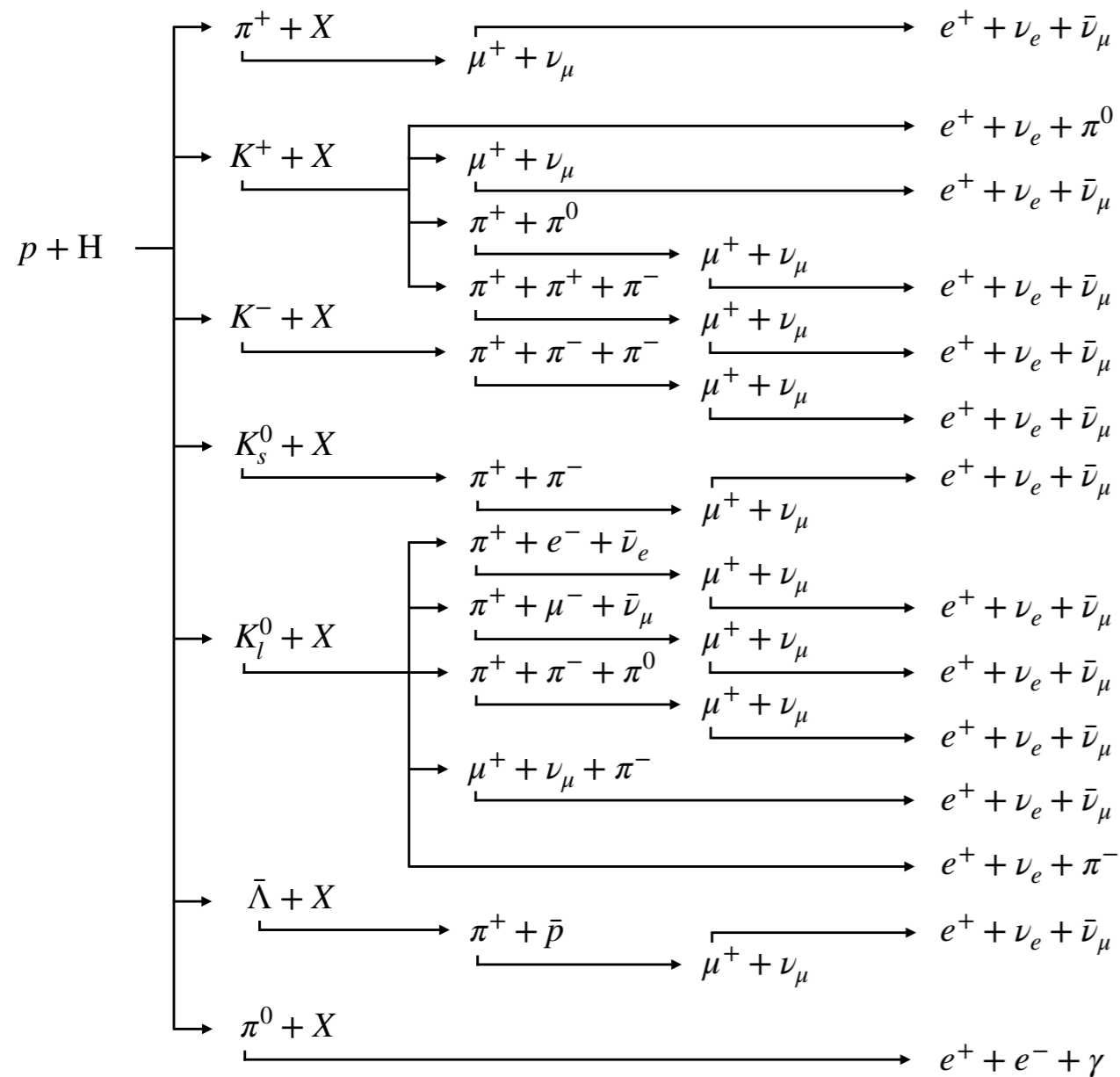
Sub-GeV antiprotons will be measured in 2023 (and 2025, 2027)
by GAPS. Robust predictions are needed:
cross sections, propagation, solar modulation

The case for

Positrons (e^+)

e^+ production channels

$$q_{ij}(T_{e^+}) = 4\pi n_{\text{ISM},j} \int dT_i \phi_i(T_i) \frac{d\sigma_{ij}}{dT_{e^+}}(T_i, T_{e^+})$$



We include all these contributions.

Similarly for collisions with nuclei.

We repeat ALL the analysis for e^- under charge conjugation

The e^\pm production chain from π^\pm production

$$\frac{d\sigma_{ij}}{dT_{e^\pm}}(T_i, T_{e^\pm}) = \int dT_{\pi^\pm} \frac{d\sigma_{ij}}{dT_{\pi^\pm}}(T_i, T_{\pi^\pm}) P(T_{\pi^\pm}, T_{e^\pm})$$

Integral over the pion production cross section convolved with the probability density function P

$$\frac{d\sigma_{ij}}{dT_{\pi^\pm}}(T_i, T_{\pi^\pm}) = p_{\pi^\pm} \int d\Omega \sigma_{\text{inv}}^{(ij)}(T_i, T_{\pi^\pm}, \theta)$$

The pion production cross section is the integral of the Lorentz Invariant cross section over scattering angle (or p_T)

$$\sigma_{\text{inv}}^{(ij)} = E_{\pi^\pm} \frac{d^3\sigma_{ij}}{dp_{\pi^\pm}^3}$$

← data

A fit is performed on the σ_{inv} data

L. Orusa, M. Di Mauro, FD, M. Korsmeier PRD 2022

Experiment	\sqrt{s} [GeV]	σ_{inv}	n	Ref.
NA49	17.3	×	×	[22]
ALICE	900	×	-	[23]
CMS	900, 2760, 7000, 13000	×	-	[24, 25]
Antinucci	π^+ (3.0, 3.5, 4.9, 5.0, 6.1, 6.8)	-	×	[26]
	π^- (3.0, 3.5, 4.9, 5.0, 6.1, 6.8)	-	×	[26]
	K^+ (2.8, 3.0, 3.2, 5.0, 6.1, 6.8)	-	×	[26]
	K^- (4.9, 5.0, 6.1, 6.8)	-	×	[26]
NA61	6.3, 7.7, 8.8, 12.3, 17.3	-	×	[21]

We use data on σ_{inv} , the multiplicity n or both.

Analytical formulae for $e\pm$ production XS

L. Orusa, M. Di Mauro, FD, M. Korsmeier PRD 2022

The procedure is fully data driven

$$\sigma_{\text{inv}} = \sigma_0(s) c_1 \left[F_p(s, p_T, x_R) + F_r(p_T, x_R) \right] A(s),$$

$$F_p(s, p_T, x_R) = (1 - x_R)^{c_2} \exp(-c_3 x_R) p_T^{c_4} \quad (8)$$
$$\times \exp \left[-c_5 \sqrt{s/s_0}^{c_6} \left(\sqrt{p_T^2 + m_\pi^2} - m_\pi \right)^{c_7 \sqrt{s/s_0}^{c_6}} \right],$$

$$F_r(p_T, x_R) = (1 - x_R)^{c_8}$$
$$\times \exp \left[-c_9 p_T - \left(\frac{|p_T - c_{10}|}{c_{11}} \right)^{c_{12}} \right]$$
$$\times \left[c_{13} \exp(-c_{14} p_T^{c_{15}} x_R) + \right.$$
$$\left. + c_{16} \exp \left(- \left(\frac{|x_R - c_{17}|}{c_{18}} \right)^{c_{19}} \right) \right]$$

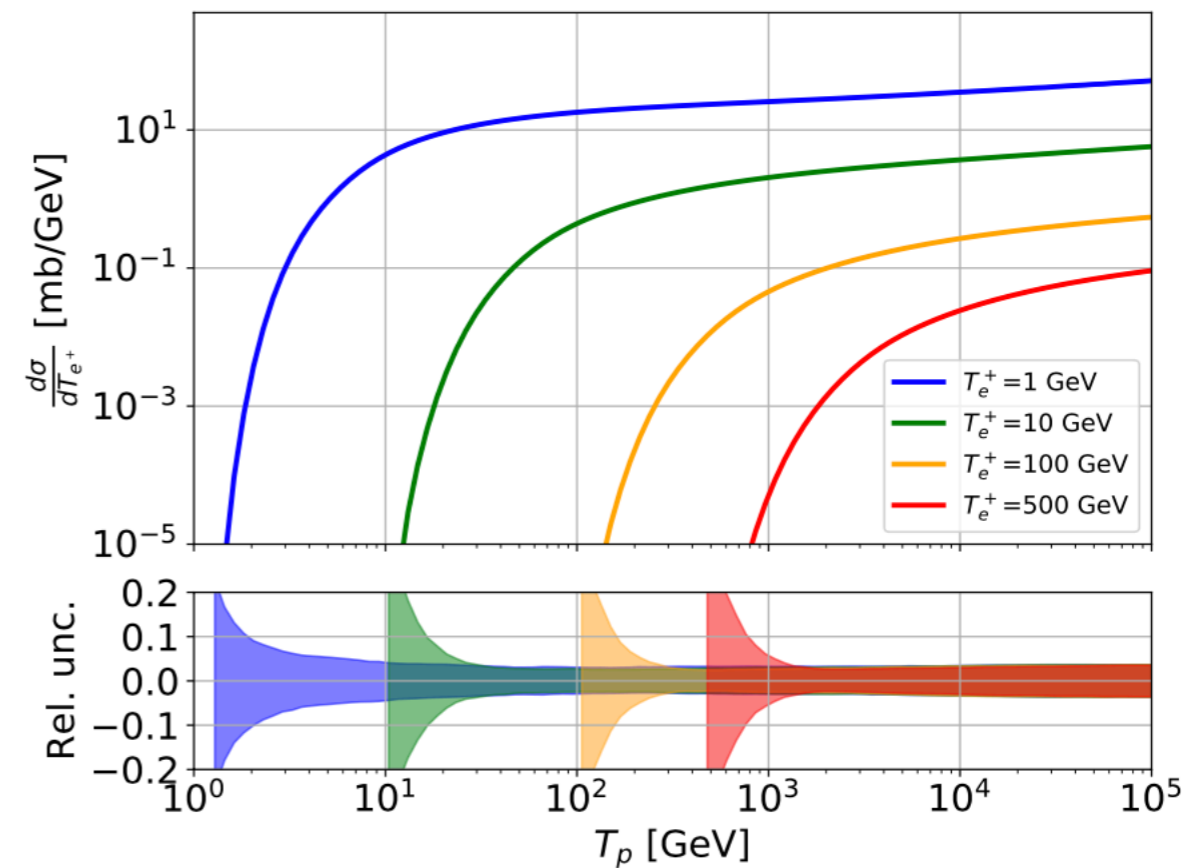
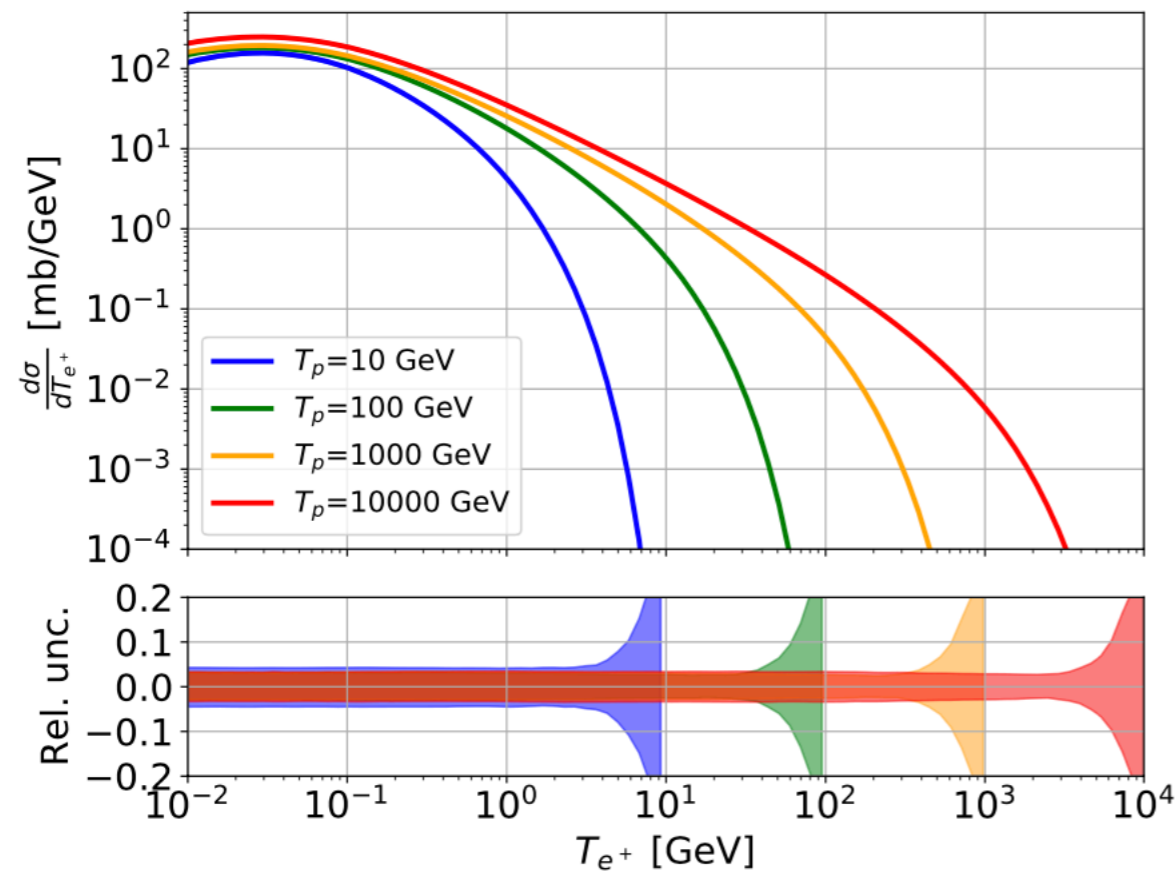
$$A(s) = \frac{1 + \left(\sqrt{s/c_{20}} \right)^{c_{21} - c_{22}}}{1 + \left(\sqrt{s_0/c_{20}} \right)^{c_{21} - c_{22}}} \left(\sqrt{\frac{s}{s_0}} \right)^{c_{22}}$$

F_s and F_r mainly driven by NA49 data

High energy behavior $A(s)$ tested on CMS and ALICE data

Results on the σ_{inv} for π^+ production

L. Orusa, M. Di Mauro, FD, M. Korsmeier PRD 2022

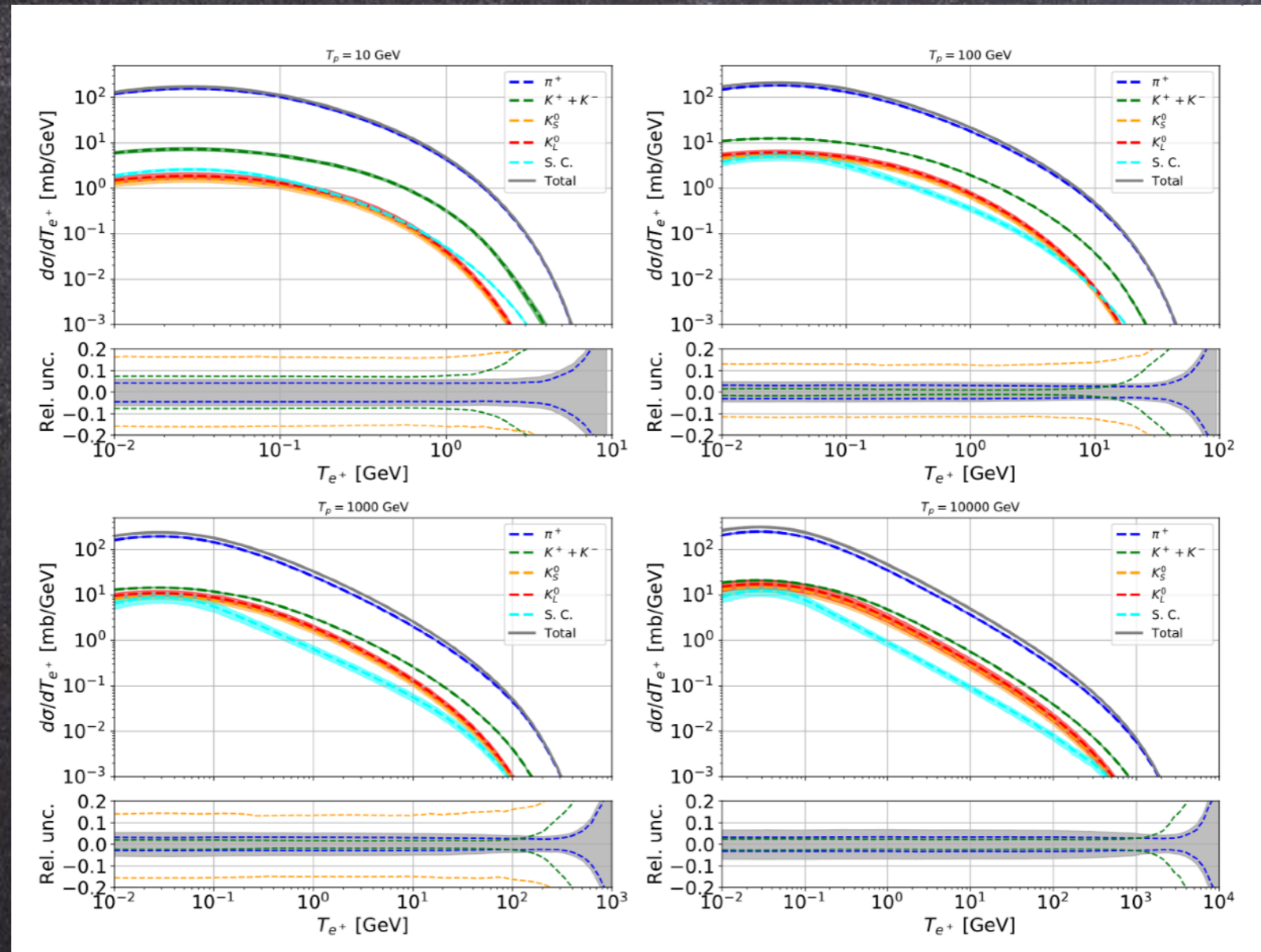


Data are fitted with very small uncertainties

Our parameterizations result appropriate, data are very precise

Total cross section from $pp \rightarrow e^+ + X$

L. Orusa, M. Di Mauro, FD, M. Korsmeier PRD 2022

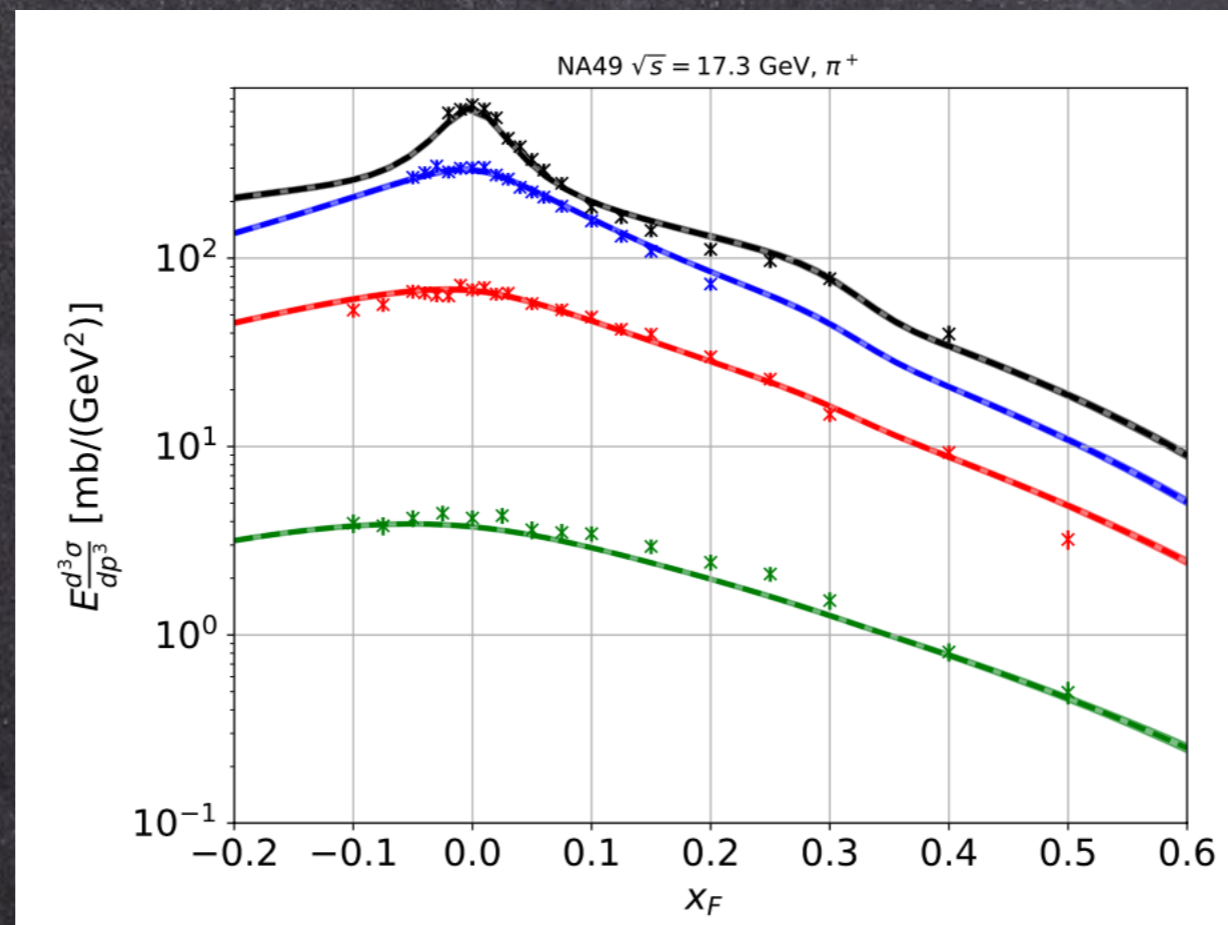


All channels contributing $>0.5\%$ are included.
Uncertainty globally contained to $<10\%$

Effect of scattering off nuclei

L. Orusa, M. Di Mauro, FD, M. Korsmeier PRD 2022

We need a model for the scattering involving He.
No data are there. We rely on NA49 $p+C \rightarrow e^++X$ data



Uncertainty is small, but very likely is not true

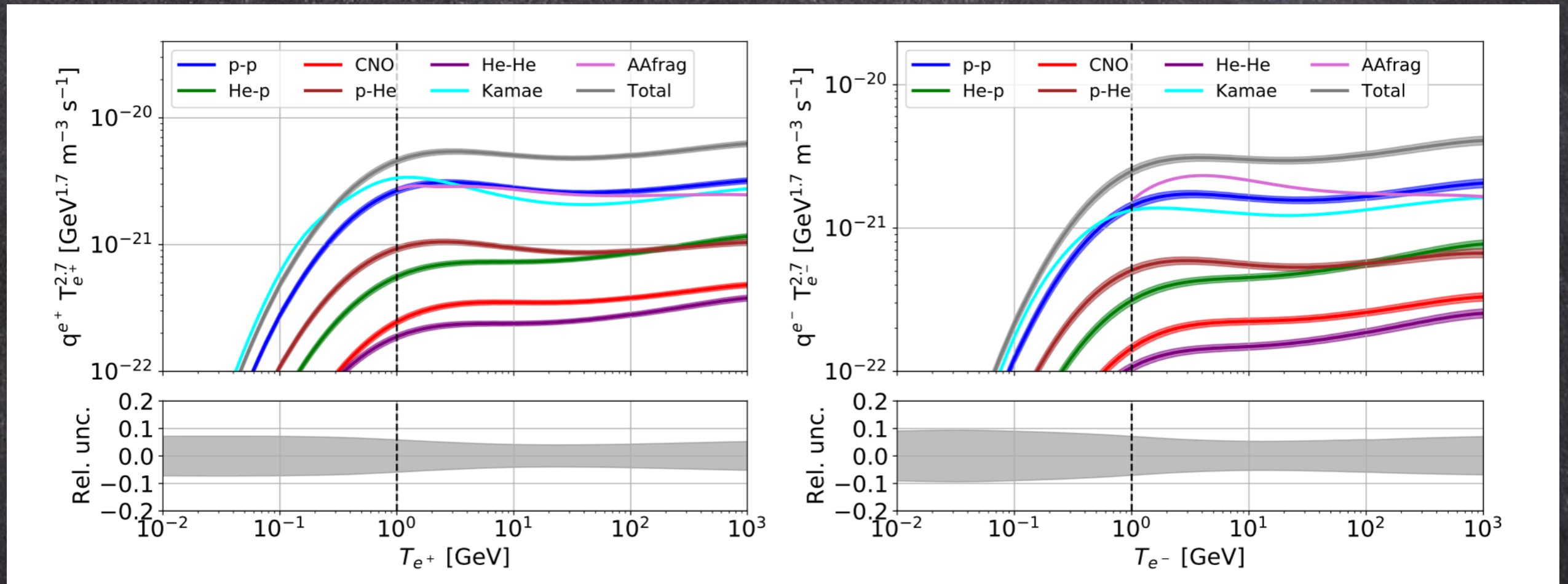
Data on He are necessary

Final results on e^+ cross section

L. Orusa, M. Di Mauro, FD, M. Korsmeier PRD 2022

Positrons

Electrons



Production cross section is now known with 7-8% uncertainty above 1 GeV. Below we extrapolate.

Comparison with MonteCarlo computations is done for p-p. Similar results for e-.

Comparison with Monte Carlo generators

Koldobskiy et al., PRD 2021, 2110.00496

Results with Aafrag

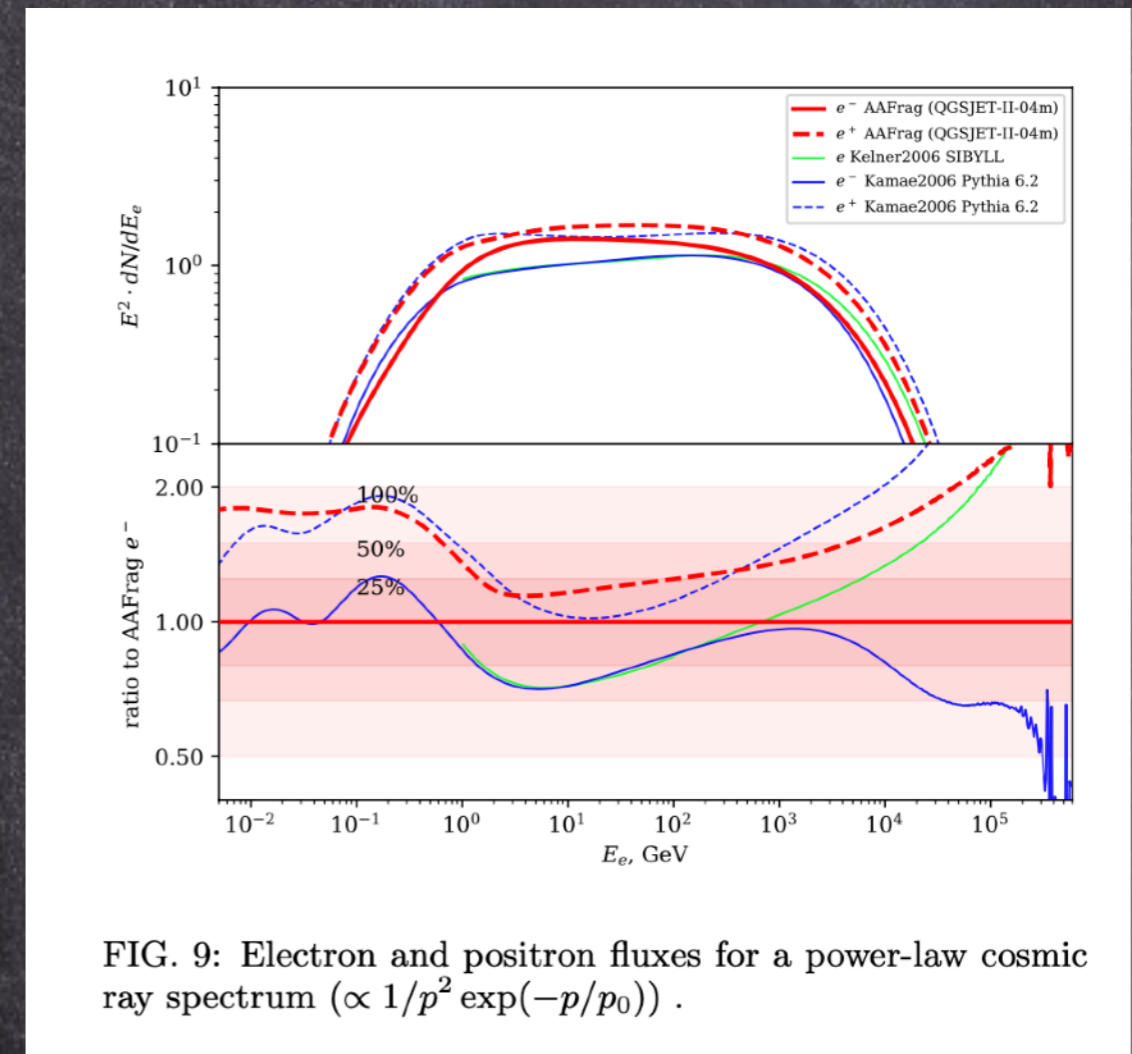
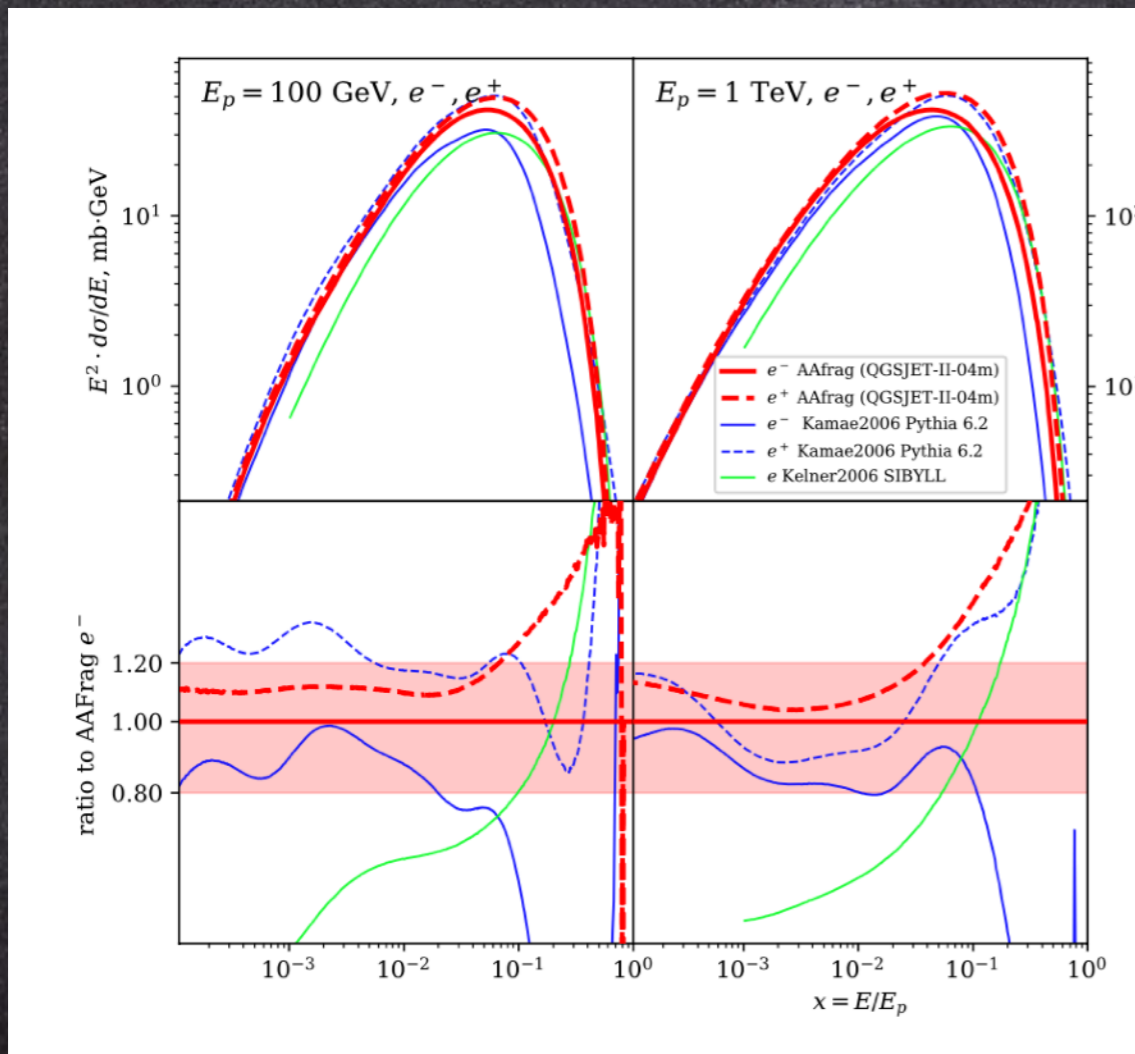
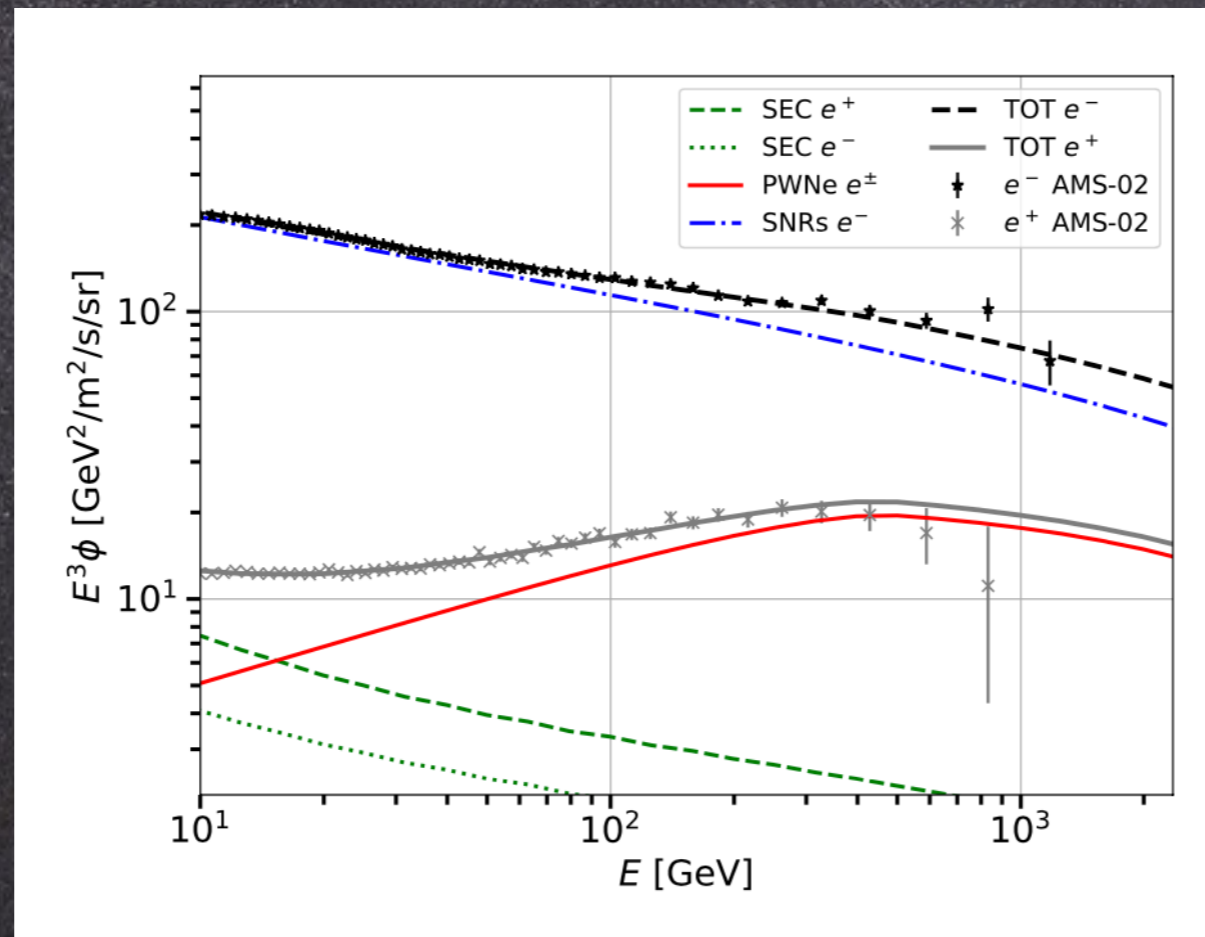


FIG. 9: Electron and positron fluxes for a power-law cosmic ray spectrum ($\propto 1/p^2 \exp(-p/p_0)$).

Different MC modelings lead to considerable differences in the Production cross section, and consequently on the source spectrum

The role of e^\pm secondaries

M. Di Mauro, FD, S. Manconi PRD 2021



e^+ secondaries contribute significantly to shape the spectrum at Earth.

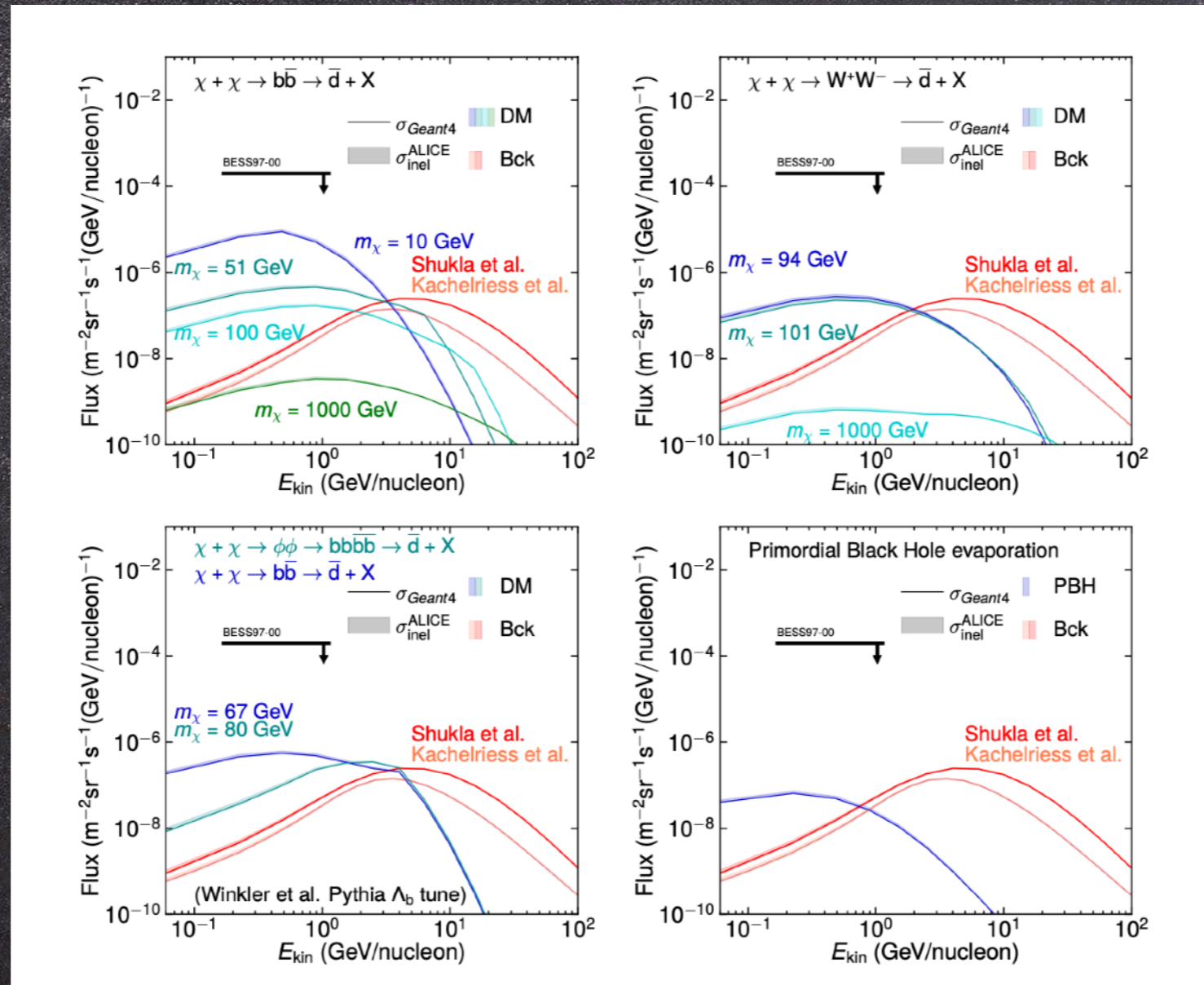
The flux in the GeV region is likely dominated by secondaries
A PRIMARY component is surely there at high energies

The case for Antideuterons

See M. Kachelriess' talk

Antideuteron perspectives

Serksnyte et al, PRD 2022



Low energy window keeps being a discovery field
Uncertainties on P_c is $\pm 70\%$

Wishes' List

Partial, and personal

1. Low energy ($0.1 < T_{p\bar{p}} < 10$ GeV) antiprotons from p-p
 2. Antideuteron fusion at low energies (p beam $\sim 10-10^2$ GeV)
 3. $p+\text{He} \rightarrow e^++X$ ($p+\text{He} \rightarrow \pi^++X$)
 4. $^{12}\text{C}+p \rightarrow \text{LiBeB}$ fragments with isotopes
- + many more!

Conclusions

Great efforts to better understand nuclei and antinuclei in CRS:
theory models, data from space, data from colliders.

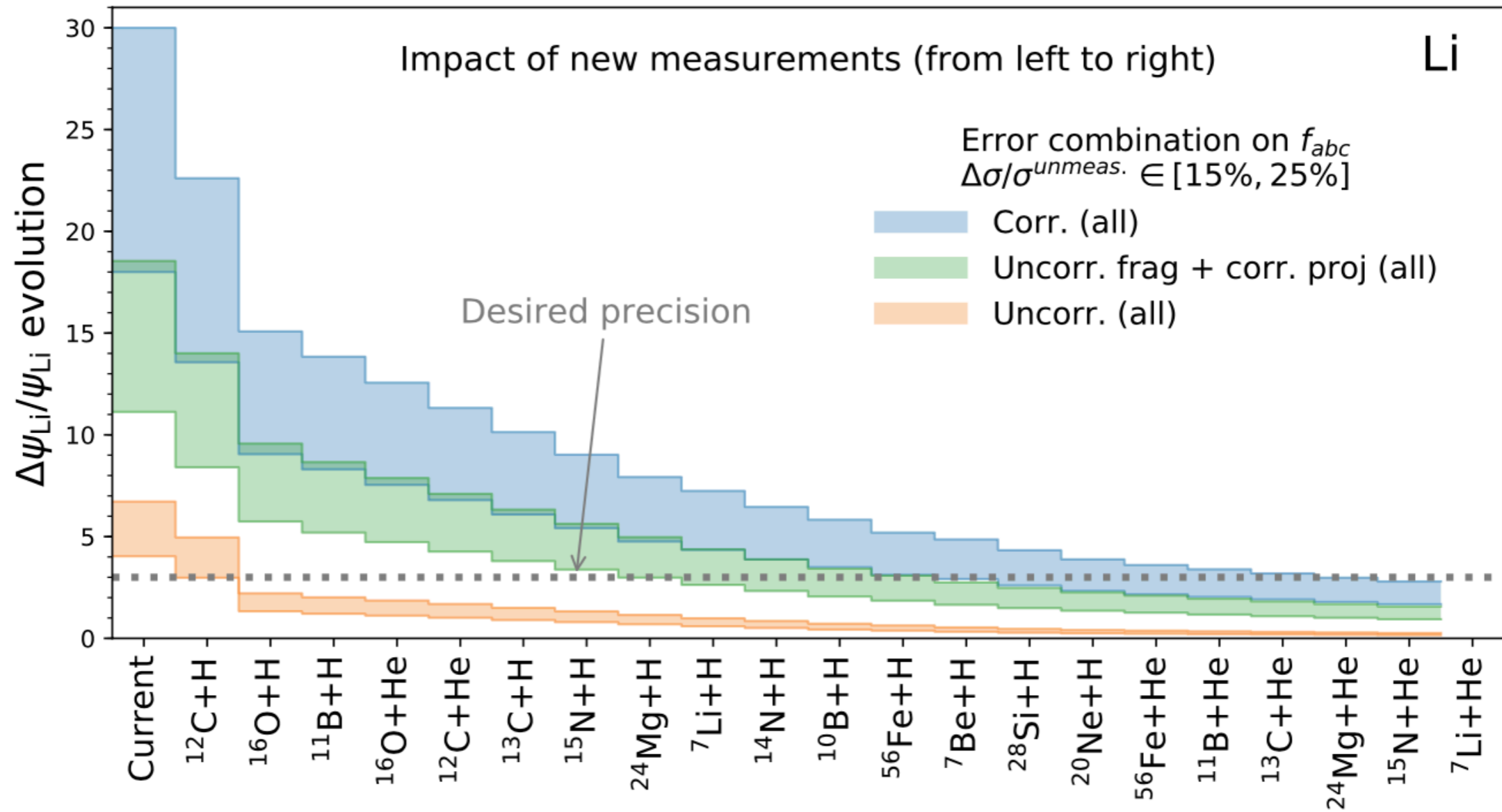
Data from space are actually hampered by lack of precise ($<10\%$) cross
section: nuclei, isotopes, antimatter, γ s

Data from colliders are highly desirable.

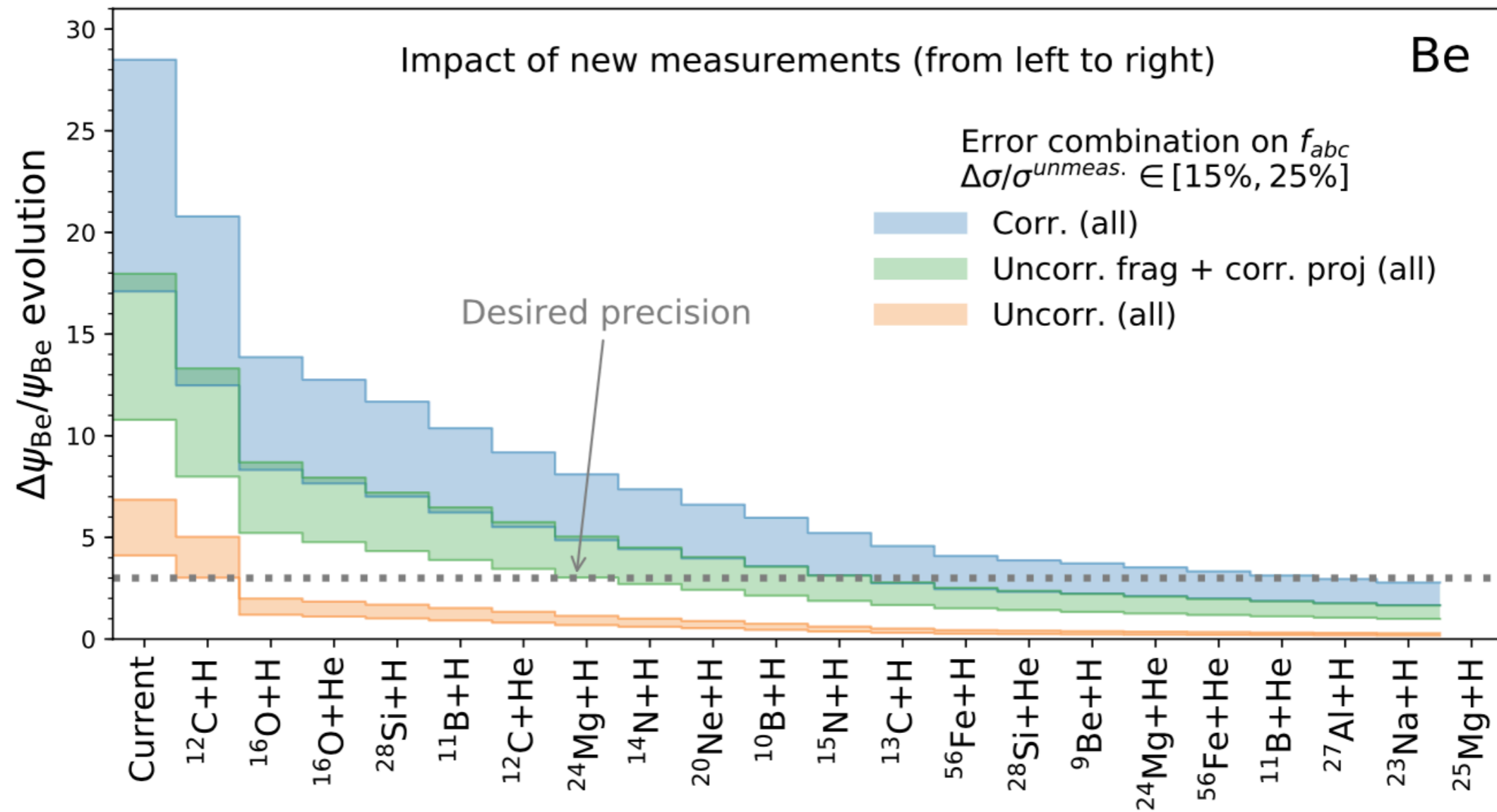
A specific receipt can be provided by the astroparticle community

Most relevant physics cases

Improve Lithium production cross sections



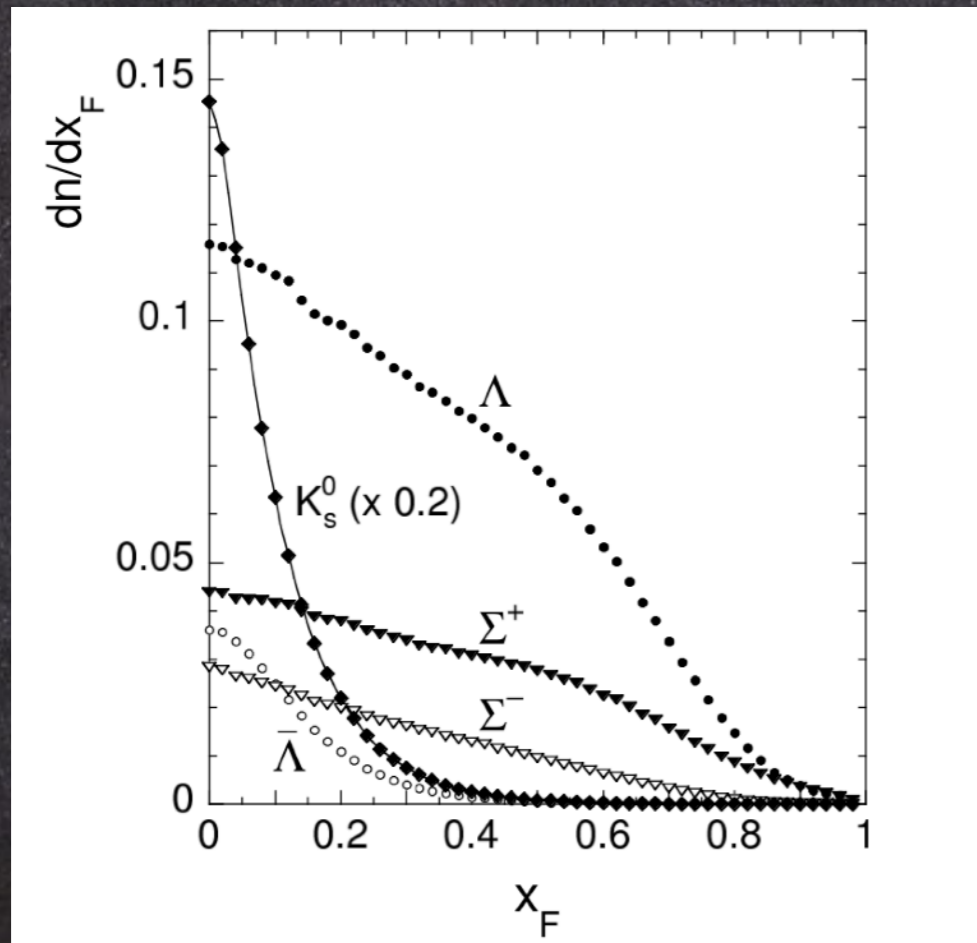
Improve Beryllium production cross sections



Data correction for feed-down

The pion production cross section can contain (or not) the pions from weak decays of strange particles.

C. Alt et al., Eur. Phys. J. C, 2005

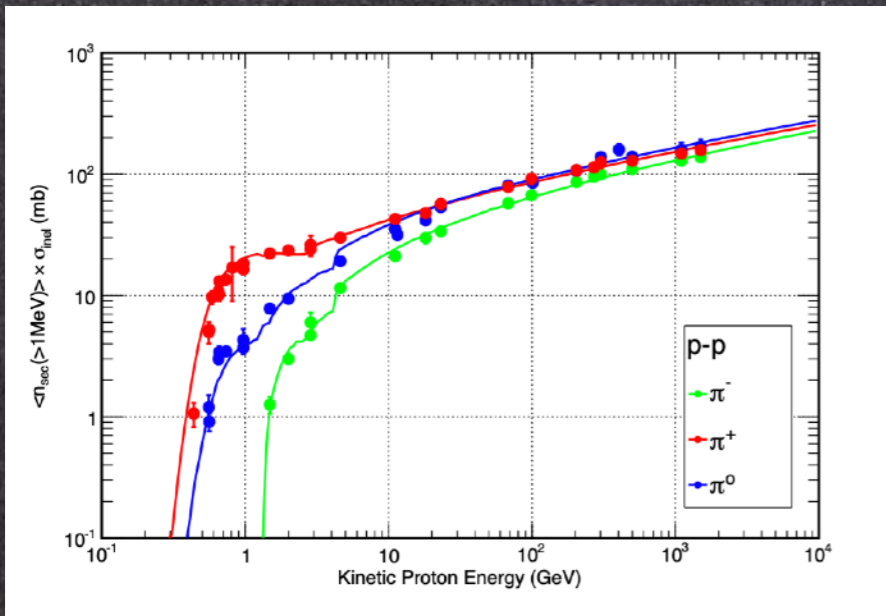


Almost all the data except the older ones are feed-down corrected. When not, we correct for it.

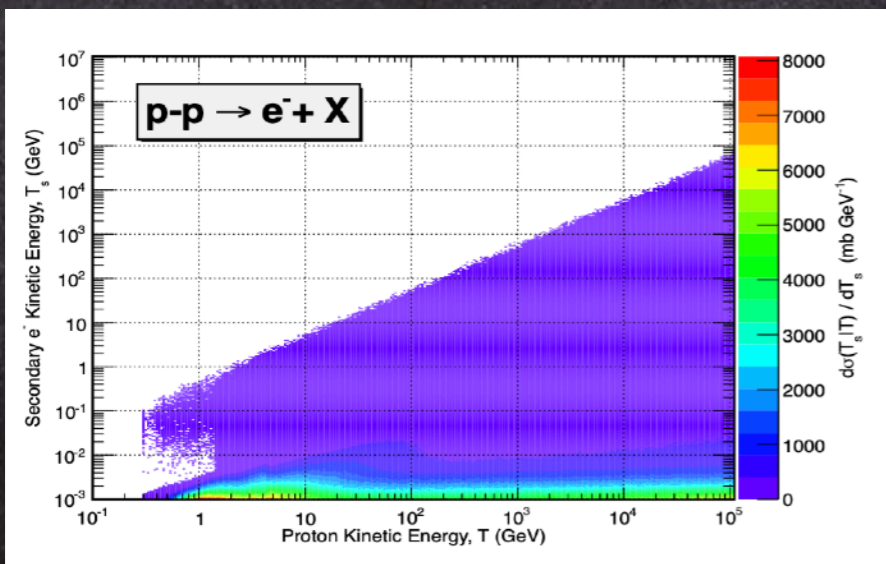
NA49 p_T integrated, MC

Fluka MC generator

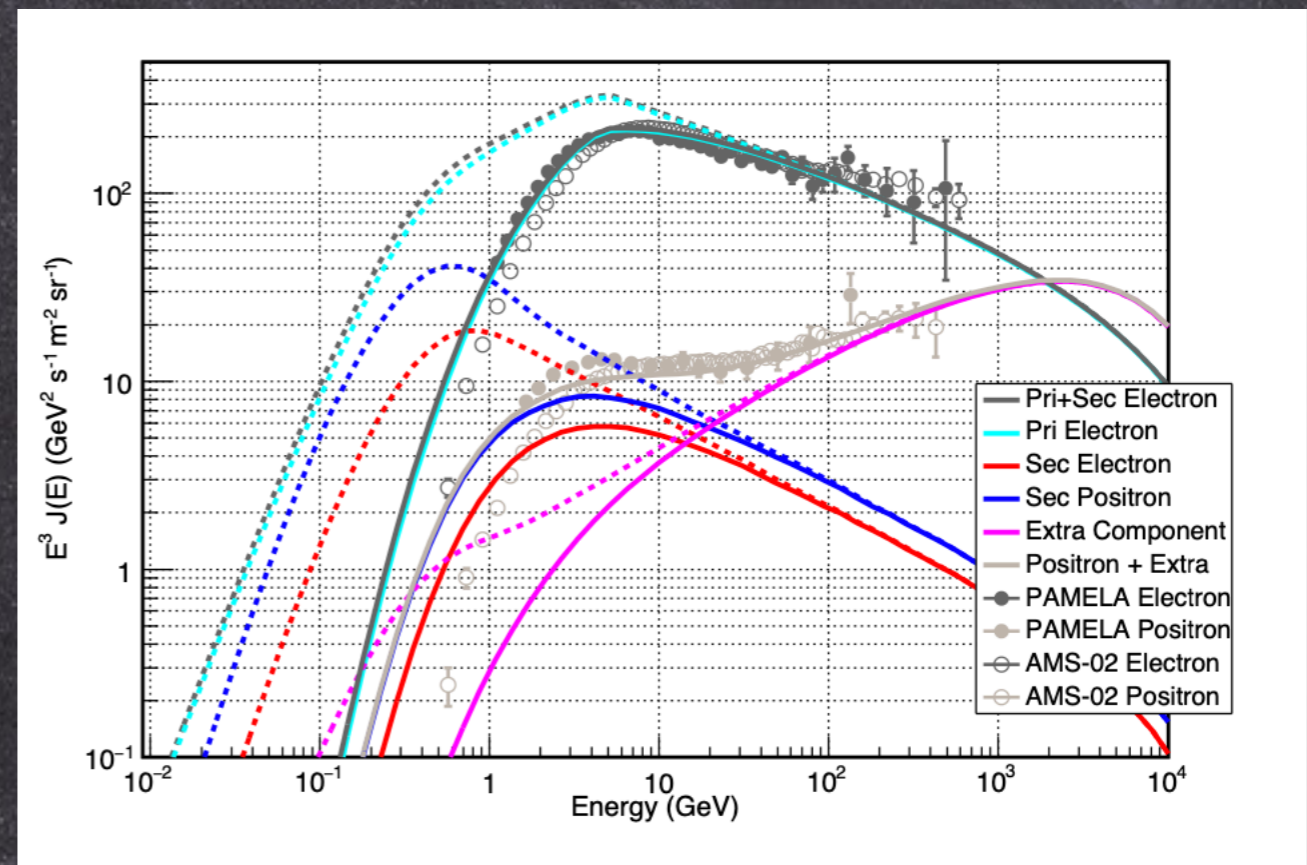
N. Mazziotta+, AP 2017



Points are from Dermer 1986



T_e is severely degraded from Projectile energy



Propagated e^+ and e^- w.r.t. data

Light nuclei: primaries and secondaries

Genolini, Moskalenko, Maurin, Unger PRC 2018

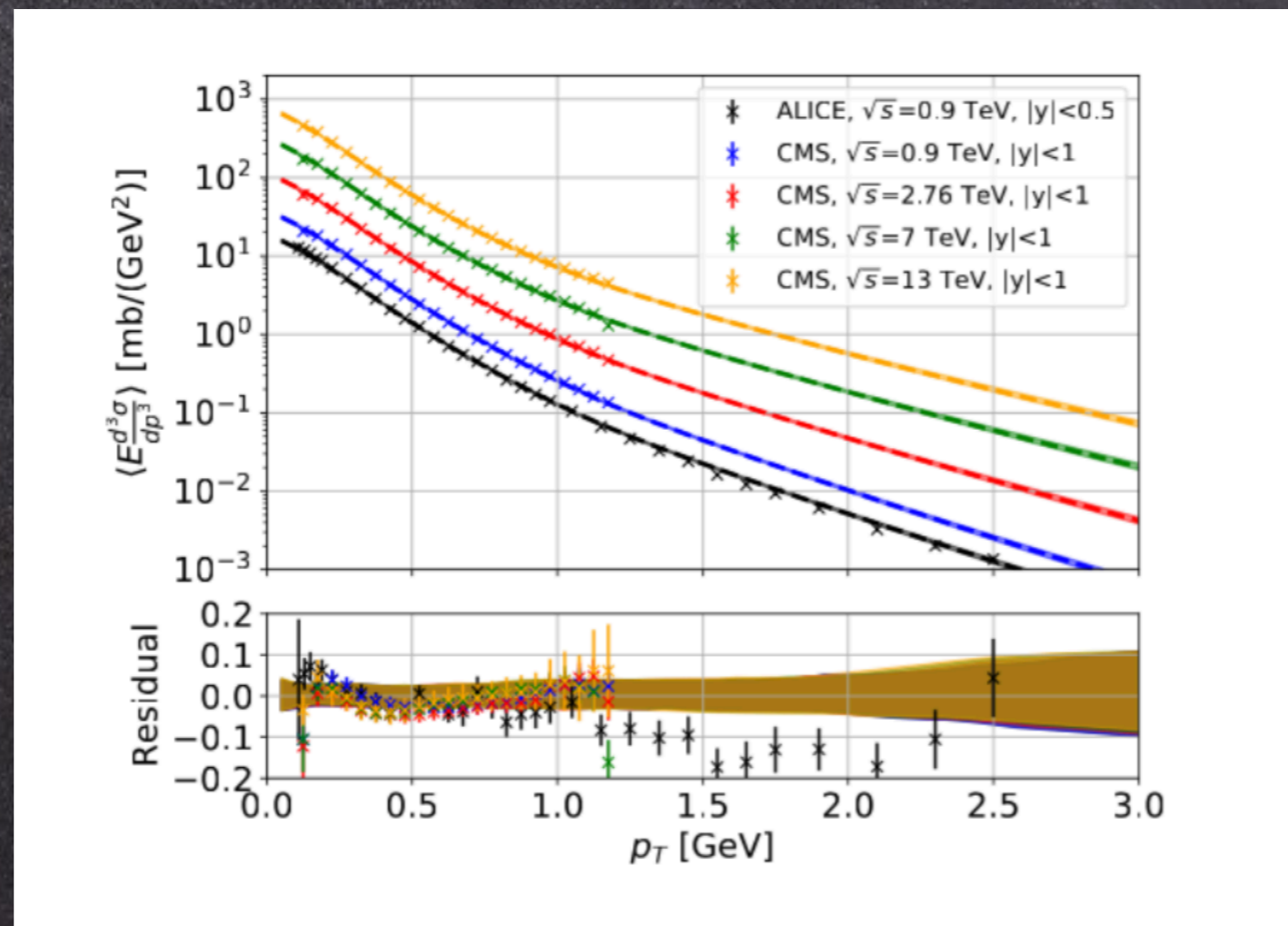
TABLE I. Fractions of primary/fragmentation/radioactive origin (w.r.t. total flux), and contributions of 1-/2-/'more-than-2' step channels (w.r.t. total secondary production) at 10 GeV/n. These numbers are independent of the propagation model if sources have the same spectral index.

CR	% isotope	% of total flux			% of multi-step secondaries		
		prim.	frag.	rad.	1	2	> 2
Li		0	100	0	66	25	9
	(56%) ${}^6\text{Li}$	0	100	0	66	25	9
	(44%) ${}^7\text{Li}$	0	100	0	66	26	8
Be		0	100	0	73	20	7
	(63%) ${}^7\text{Be}$	0	100	0	78	17	6
	(30%) ${}^9\text{Be}$	0	100	0	65	26	9
	(6%) ${}^{10}\text{Be}$	0	100	0	66	26	7
B		0	95	5	79	17	5
	(33%) ${}^{10}\text{B}$	0	85	15	70	24	6
	(67%) ${}^{11}\text{B}$	0	100	0	82	14	4
C		79	21	0	77	17	5
	(90%) ${}^{12}\text{C}$	88	12	0	72	21	6
	(10%) ${}^{13}\text{C}$	7	93	0	83	13	4
	(0.02%) ${}^{14}\text{C}$	0	100	0	56	35	9
N		27	72	2	87	9	4
	(54%) ${}^{14}\text{N}$	49	48	3	83	13	4
	(46%) ${}^{15}\text{N}$	0	100	0	89	7	3

Results at large \sqrt{s}

L. Orusa, M. Di Mauro, FD, M. Korsmeier PRD 2022

We use σ_{inv} or multiplicity



Uncertainties between 5% and 10% – most relevant is 5% at low p_T

Antimatter or γ -rays sources from DARK MATTER

Annihilation

$$Q_{\text{ann}}(\vec{x}, E) = \epsilon \left(\frac{\rho(\vec{x})}{m_{\text{DM}}} \right)^2 \sum_f \langle \sigma v \rangle_f \frac{dN_{e^\pm}^f}{dE}$$

Decay

$$Q_{\text{dec}}(\vec{x}, E) = \left(\frac{\rho(\vec{x})}{m_{\text{DM}}} \right) \sum_f \Gamma_f \frac{dN_{e^\pm}^f}{dE}$$

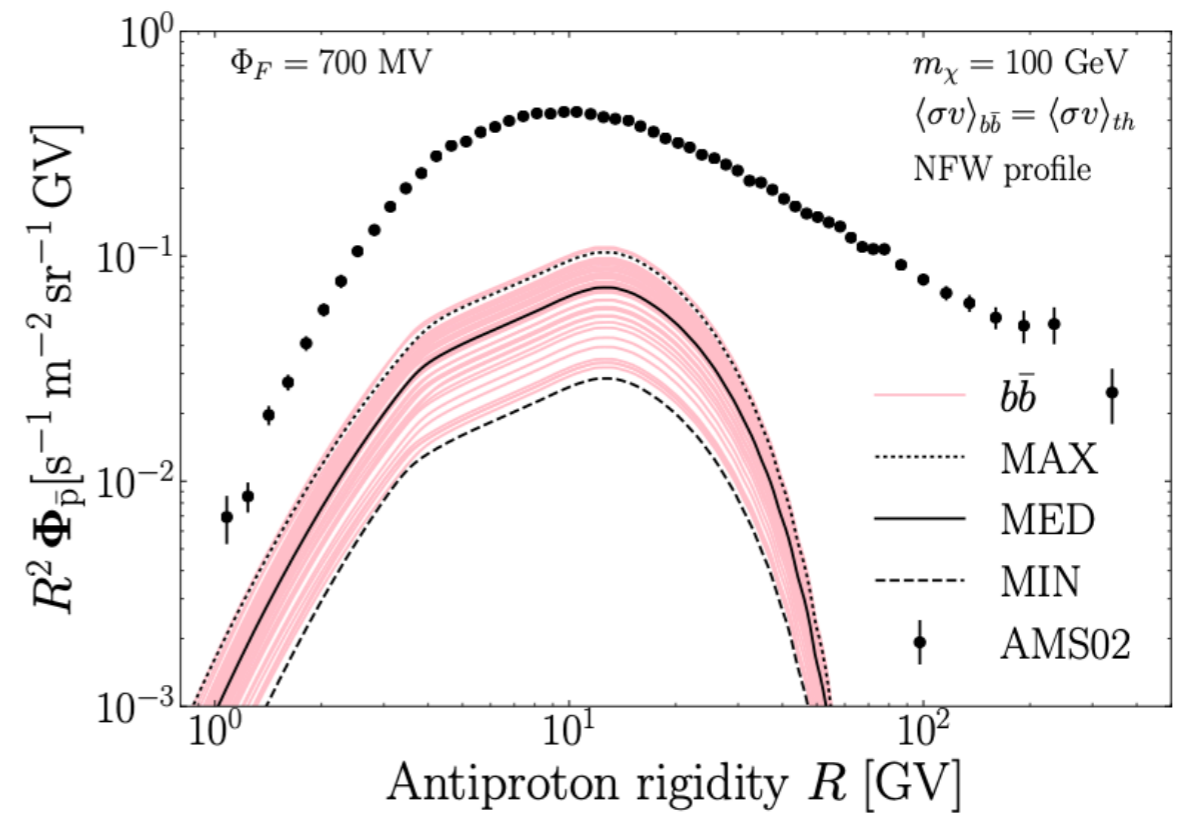
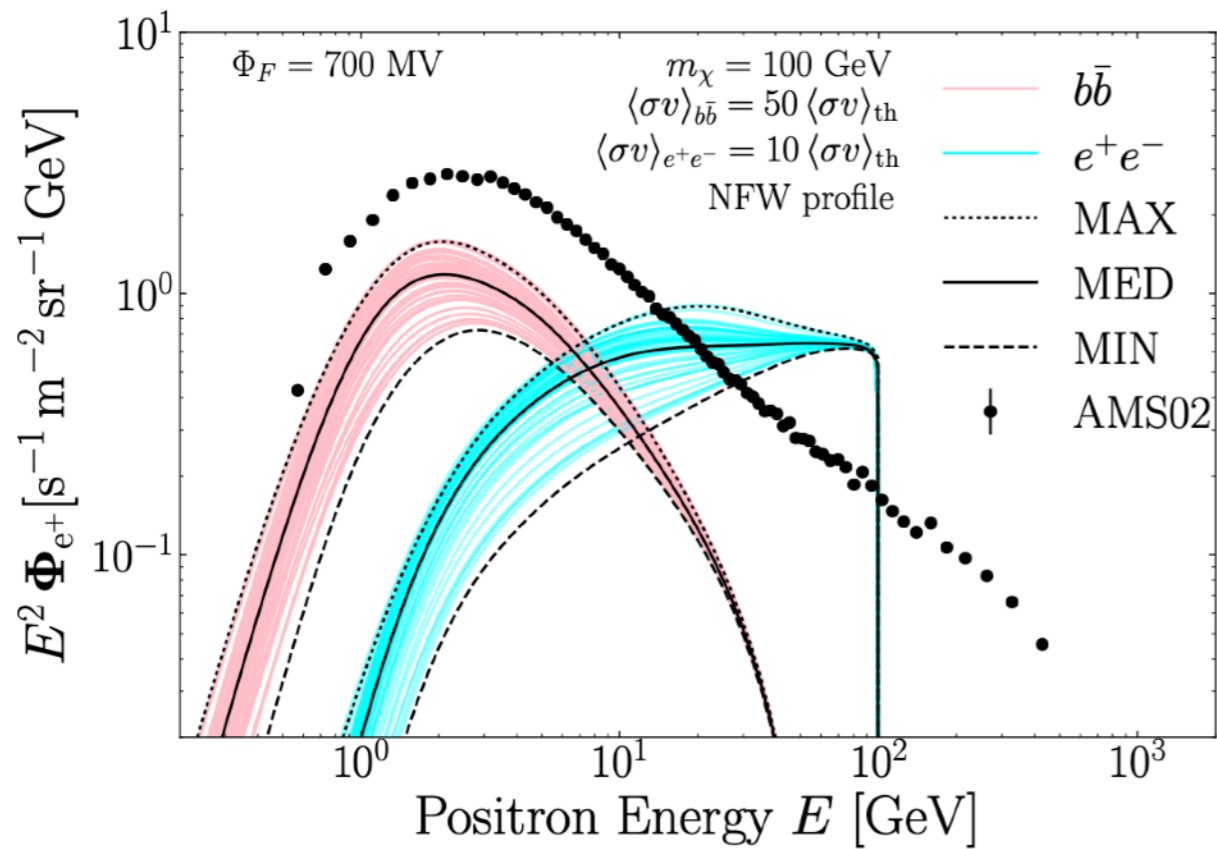
- ρ DM density in the halo of the MW
- m_{DM} DM mass
- $\langle \sigma v \rangle$ thermally averaged annihilation cross section in SM channel f
- Γ DM decay time
- e^+ , e^- energy spectrum generated in a single annihilation or decay event

Annihilations take place in the whole diffusive halo

Effect of galactic propagation

Genolini+ 2103.04108

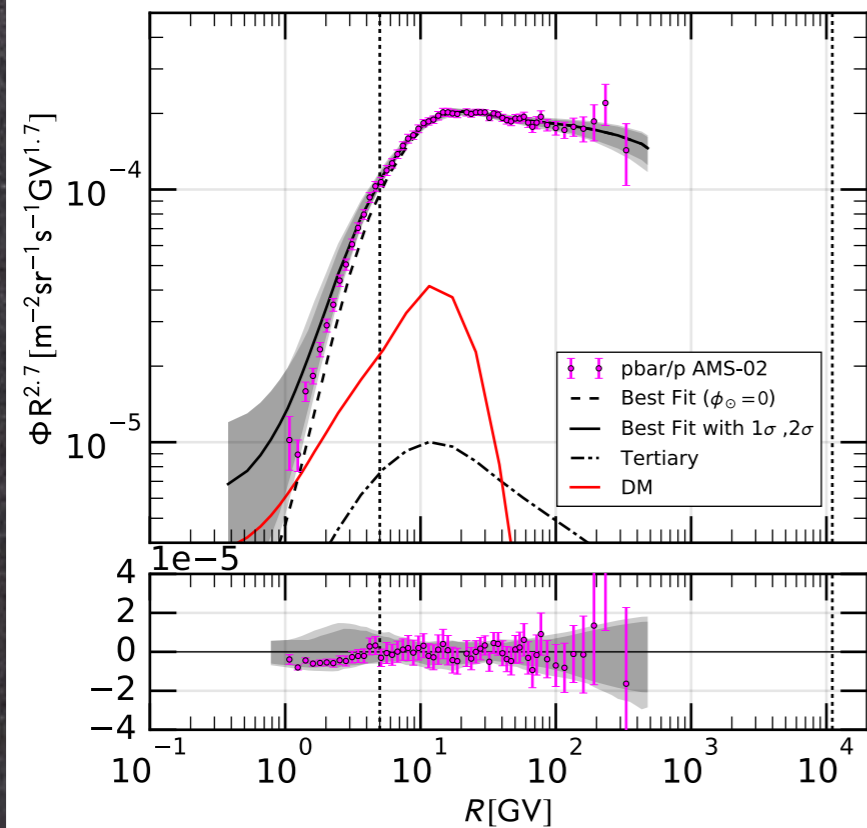
Galactic propagation has strong impact on Dark Matter induced fluxes



New AMS-02 sec/prim data allow reduction of propagation uncertainties

Possible contribution from dark matter

Cuoco, Korsmeier, Kraemer PRL 2017



Antiproton data are so precise that permit to set strong upper bounds on the dark matter annihilation cross section, or to improve the fit w.r.t. to the secondaries alone adding a fine DM contribution

Heisig, Korsmeier, Winkler PRD2020 2020

Derivation of covariance matrix for systematic errors (dominated by $p(\bar{p})C$ absorption cross section) The significance for DM drops below 1sigma

